UNIVERSIDADE FEDERAL DO RIO GRANDE DO SUL
INSTITUTO DE FÍSICA
DEPARTAMENTO DE ASTRONOMIA

Self-consistent nebular emission and stellar population analysis of jellyfish galaxies

Gabriel Maciel Azevedo

Trabalho de Conclusão de Curso apresentado à Comição de Graduação em Física do Instituto de Física da Universidade Federal do Rio Grande do Sul sob orientação da Prof. Dr. Ana Leonor Chies Santiago Santos e do Prof. Dr. Rogério Riffel, como parte dos requisitos para a obtenção do grau de Bacharel em Física - ênfase em Astrofísica.

Porto Alegre, RS, Brasil
May, 2021

"As flores brotam e morrem, as estrelas brilham, mas um dia se apagarão. Tudo morre, a Terra, o Sol, a Via Láctea, e até mesmo todo esse universo não é exceção... Comparado a isso, a vida do homem é tão breve e fugidia quanto um piscar de olhos. Nesse curto instante, os homens nascem, riem, choram, lutam, sofrem, festejam, lamentam, odeiam pessoas e amam outras. Tudo é transitório, e em seguida todos caem no sono eterno chamado morte."

Masami Kurumada (Shaka, Cavaleiros do Zodíaco, ep 124)

Agradecimentos

Agradeço à minha família por todo apoio e carinho ao longo desses anos, e em especial aos meus pais por sempre terem me incentivado a me dedicar aos estudos e continuamente trabalhado para me prover educação de qualidade.

Agradeço à minha namorada Caroline, por ter me acompanhado, me divertido e me ajudado durante esses últimos semestres de graduação.

Agradeço aos meus amigos antigos por alegrarem meus dias ao longo de tantos anos, e em especial ao Eduardo, que me incentivou a seguir com minha escolha de profissão.

Agradeço aos colegas de curso e aos amigos feitos dentro da universidade, que tornaram minha graduação mais divertida e me ajudaram incontáveis vezes, especialmente ao Augusto, ao Gabriel Roier, ao João Pedro, à Fernanda e ao Rodrigo, aqueles que mais me ajudaram a resolver dificuldades na minha pesquisa.

Agradeço à professra Ana e ao professor Rogério por me introduzirem e me guiarem com sabedoria na vida de cientista, e a todos os demais professores do instituto que me transmitiram uma enorme quantidade de conhecimento.

Gostaria de agradecer ao colaborador Jean, pela disposição a me ajudar e me ensinar sobre uma ferramenta essencial para esse trabalho.

Ao CNPq, por financiar minha iniciação científica.

Agradeço àqueles que porventura esqueci de mencionar e contribuíram direta ou indiretamente para que esse trabalho fosse concluído.

Resumo

Galáxias em movimento em um ambiente denso, como grupos e aglomerados de galáxias, são sujeitas a uma pressão de arrasto causada pelo gás intra-aglomerado. Em dadas situações ocorre de a pressão remover o gás da galáxia, fenômeno chamado de *ram pressure stripping*, e originar as galáxias *jellyfish*, as quais são caracterizadas por uma assimetria unilateral e estruturas de caudas de gás com formação estelar. Nesse trabalho nós realizamos síntese de população estelar espacialmente resolvida de 19 *jellyfish* observadas pelo levantamento GASP utilizando o instrumento de espectroscopia de campo integral MUSE. A síntese é um método que consiste em calcular a combinação de populações estelares (populações de estrelas com diferentes idades e metalicidades) que melhor reproduz o espectro de energia observado. A implementação desse método foi feita com o código FADO, que além de sintetizar o espectro estelar, usa como condição de contorno extra o espectro nebular, calculado a partir de diversas linhas de emissão. Nós criamos mapas com idades e metalicidades médias, emissão de H_α e densidade superficial de taxa de formação estelar de todas as galáxias da amostra. Apresentamos também histogramas cumulativos das frações de luz e de massa que populações de diferentes idades representam nas galáxias, bem como um histograma médio da amostra. Analisamos os resultados das sínteses com relação à intensidade do *stripping* e vimos que as galáxias mais perturbadas têm em média populações mais jovens que aquelas com leves assimetrias e são em média menos metálicas se comparadas às galáxias com *stripping* intermediário, enquanto essas têm metalicidades médias menores ou semelhantes às com leves assimetrias. O estudo das galáxias no espaço de fases revelou que as *jellyfish* na região virializada de seus aglomerados hospedeiros tendem a ter idades médias maiores ($\gtrsim$ 2 Gyr para as médias pesadas por luz e $\gtrsim$ 3 Gyr para as pesadas por massa) que aquelas na região de recente entrada no aglomerado.

Abstract

Galaxies moving in dense environments, such as groups and clusters of galaxies, are subject to a ram pressure caused by the intracluster gas. In certain situations, such pressure removes the gas from the galaxy, giving rise to a phenomenon called ram pressure stripping, and originating the jellyfish galaxies. These are characterized by unilateral asymmetry and tail structures of gas and star formation. In this work we performed spatially resolved stellar population synthesis of 19 jellyfish galaxies observed by the GAs Stripping Phenomena in galaxies with MUSE (GASP) survey with the integral field spectrograph MUSE. The spectral population synthesis (SPS) is a method that consists of computing the linear combination of stellar populations (populations of stars with different ages and metallicities) which best reproduces the spectral energy distribution of an observed galaxy. The implementation of the method has been done with the SPS code FADO (Fitting Analysis using Differential evolution Optimization), which besides synthesizing the stellar spectrum, has the nebular spectra computed from various emission lines, as an additional boundary condition. We created 2D morphology maps of mean stellar ages and metallicities, H_α emission, and star formation rate surface densities for all sample galaxies. We also present cumulative histograms with the fractions of light and mass of populations with different ages contained in the galaxies and a mean histogram of the sample. We analyzed the synthesis results concerning the intensity of the stripping and observed that the most disturbing galaxies have, on average, younger populations than those with slight asymmetries. The most extreme cases are also, on average, less metallic than those with intermediate stripping, while these have mean metallicities more significant or similar to those with slight asymmetries. The study of the jellyfish galaxies on the phase space reveals that those in the virialized region of their host clusters tend to have mean ages greater ($\gtrsim$ 2 Gyr for light-weighted values and $\gtrsim$ 3 Gyr for mass-weighted ones) than those in the region of recent infall.

Press Release: As águas-vivas do espaço sideral

Há menos de um século que nós humanos temos conhecimento da existência de outras galáxias além da Via Láctea no Universo. E não são poucas, mas centenas de bilhões delas, dos mais variados formatos e tamanhos. Algumas são espirais, como a Via Láctea, algumas são elípticas e outras são irregulares, sem nenhum formato bem definido. Algumas possuem formatos tão únicos e característicos que são criadas novas classificações para encaixá-las, como é o caso das galáxias *jellyfish* (água-viva em inglês), que possuem caudas de gás e estrelas que faz com essas galáxias lembrem o animal marinho.

Muitas galáxias no Universo tendem a se agrupar em aglomerados perto de outra muito grande, de forma parecida a como os planetas se juntam ao redor do Sol ou como as estrelas se aglomeram em nossa galáxia. Nesses aglomerados, o espaço que as separa é cheio de gás. Quando uma galáxia começa a cair em direção ao centro (à maior galáxia) ela sofre uma pressão por estar se movendo rápido nesse gás que existe entre elas, igual a quando corremos e sentimos a força do vento contra o corpo. Essa pressão é chamada *pressão de arrasto*.

Entretanto, as galáxias também podem ser cheias de gás no espaço que separa as estrelas. Esse gás é muito mais facilmente afetado pela força da pressão de arrasto do que as estrelas, e pode acontecer da galáxia continuar sua queda, mas seu gás ficar pra trás e formar caudas, e é nesse contexto que surgem as galáxias *jellyfish*. O gás nas caudas então pode originar regiões de formação estelar, afinal todas as estrelas surgem à partir de uma enorme nuvem de gás e poeira que se condensa com a gravidade. Fazendo uma analogia: ao balançar um aro com sabão no ar, sua mão e o aro mal sentem resistência, mas o sabão fica pra trás e forma bolhas pelo caminho.

Uma compreensão detalhada de como as galáxias se formaram e evoluíram desde o começo do Universo é um dos pilares da astronomia moderna e processo da perda do gás nas galáxias *jellyfish* é importante para entender a evolução das galáxias no contexto de suas interações com o ambiente ao seu redor. Esse mecanismo muda não só radicalmente a forma delas, mas também outras várias características, como a taxa com que elas formam estrelas. Um grupo de astrônomos da UFRGS usa técnicas de análise baseadas em como a luz é emitida por essas galáxias para entender como acontece a formação das estrelas e quais são suas idades, entre outras medidas.

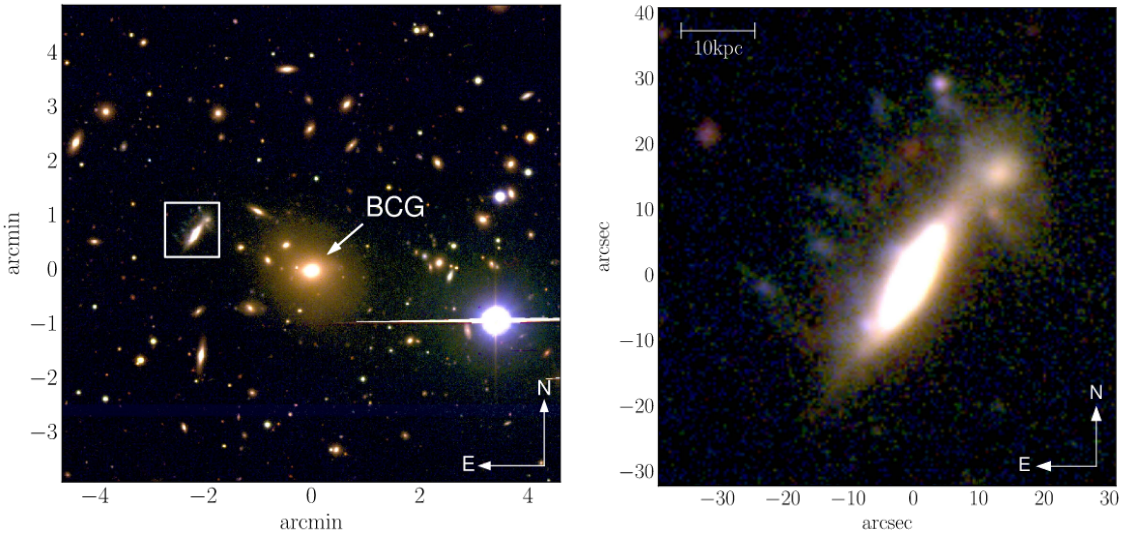

Figure 1: À esquerda, uma imagem do aglomerado A957x e da galáxia *jellyfish* JO204 (quadrado branco) caindo em direção à maior galáxia do aglomerado. À direita, uma imagem ampliada da JO204 (Gullieuszik et al., 2018).

Abbreviations

CMB: Cosmic Microwave Background
ESO: European Southern Observatory
FADO: Fitting Analysis using Differential evolution Optimization
FoV: Field of View
GASP: GAs Stripping Phenomena in galaxies with MUSE
GC: Globular Cluster
gE: Giant Elipticals
ICM: Intracluster Medium
IFS: Integral Field Spectrograph
IFU: Integral Field Units
IMF: Initial Mass Function
ISM: Interestellar Medium
MNRAS: Monthly Notices of the Royal Astronomical Society
MUSE: Multi Unit Spectroscopic Explorer
NIR: Near Infrared
PM2GC: Padova Millennium Galaxy and Group Catalogue
RPS: Ram-Pressure Stripping
SED: Spectral Energy Distribution
SFH: Star Formation History
SFR: Star Formation Rate
SPS: Stellar Population Synthesis
SSP: Simple Stellar Population
UCD: Ultra Compact Dwarf

Contents

Chapter 1

Introduction

Less than one century ago, Edwin Hubble discovered that there were other galaxies in the universe besides the Milky Way and that most of them were moving away from us (Hubble, 1925). Our Universe is inhabited by billions of galaxies and is expanding at an accelerated rate (Riess et al., 1998, Perlmutter et al., 1999). It started growing $\sim$ 13.8 billion years ago (Kozmanyan et al., 2019) from a state of extreme density and temperature, known as a singularity. It is until now enlarging its volume and spreading its matter and energy more and more.

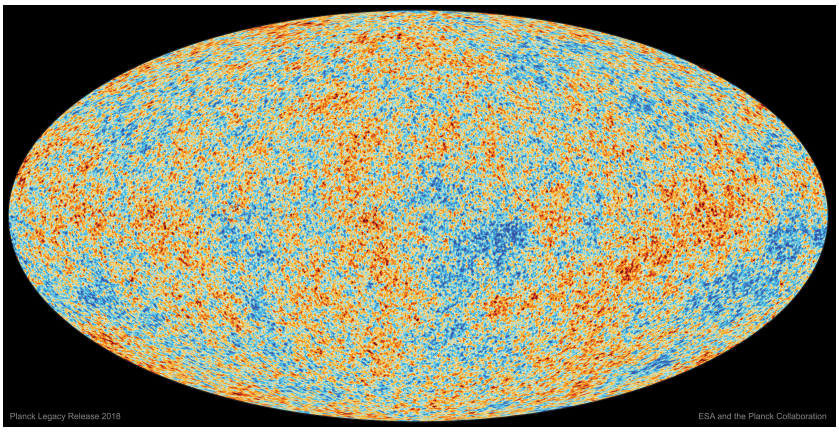

Figure 1.1: Map of the CMB along the sky obtained with the Planck satellite. The red color represents hotter regions, which are also the overdense regions.

Although the Universe is uniform in large scales (dozens of Mpc), it was not formed in a completely uniform way. For example, we can see through the cosmic microwave background (CMB), which is the remaining radiation from the early Universe (age $\sim$ 380,000 yr), that is full of areas with overdensities (see figure 1.1). This result is because the expansion allowed the gas to cool and collapse by its gravity in such regions, forming stars and later galaxies, in a hierarchical manner,

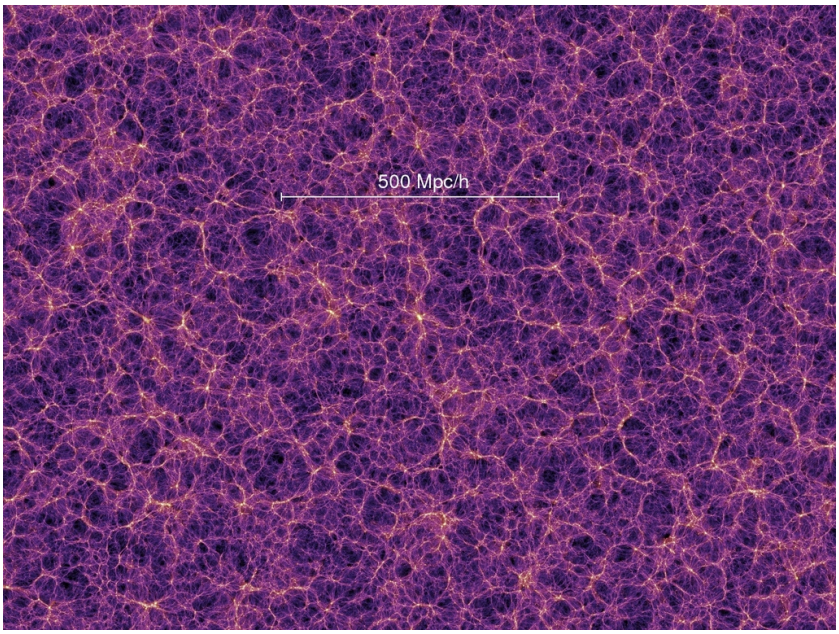

Figure 1.2: Representation of the cosmic web made with the Millennium simulation (Springel et al., 2005). The purple color represents dark matter, and the yellow one represents clusters of galaxies.

with smaller objects grouping into larger ones, giving birth to a large variety of galaxies and clusters. So, as the universe keeps expanding, there are several of those regions of gravitationally bound matter that along with the dark matter (DM) form a "spongeous" distribution over space, which is called the cosmic web (see figure 1.2). That said, *the growth of the Universe itself is wholly connected with the evolution of galaxies and clusters. It thus relies on the interest in studying the mechanisms that change these environments and their components.*

1.1 Galaxy morphology and evolution

There is a great diversity of morphological types of galaxies. In 1926 Hubble classified the known galaxies into different groups according to their shapes and colors (see figure 1.3)(Hubble, 1926). The galaxies can be separated into three bigger groups: the ellipticals, which are spheres or ellipsoids, and are dominated by old, colder, and red stars; the spirals, that present a bulge in the center and a disc with spiral arms, and are dominated by young, hotter and blue stars; and the irregulars, that do not fit the other two shapes and generally have young stars. The lenticular galaxies (S0) are also an intermediate morphology between ellipticals and spirals, which have large disks but without spiral arms and with low ongoing star formation.

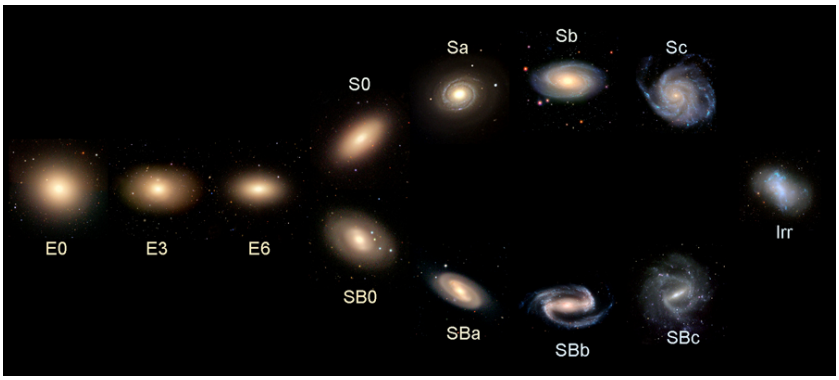

Figure 1.3: Hubble's morphology classification of galaxies. On the left are the ellipticals. On the bottom right are the barred spiral, and on the top right are the spiral galaxies without a bar. On the very right is an irregular galaxy.

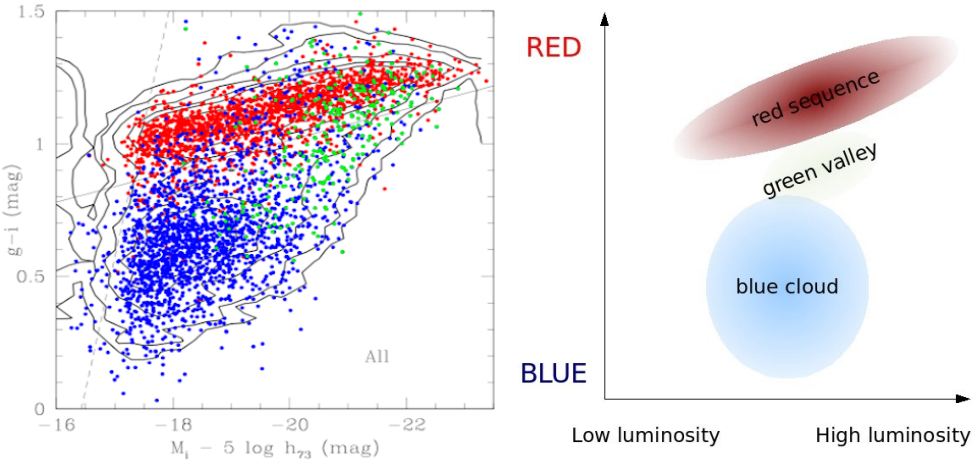

Figure 1.4: Left: galaxy color-diagram magnitude from (Gavazzi et al., 2010). Right: illustrative representation of the diagram. Credit: Joshua Schroeder.

The Hubble classification was only statistical and did not proposed and evolutionary time sequence, although one could argue that late-types have younger stellar populations and then were formed more recently, and that early-types were formed first because their stars are predominantly old. Today it is known that most galaxies started forming their stars at similar times, but the most massive stopped the star formation early. However, dwarfs seem to be still forming stars (Thomas et al., 2005). So one of the main differences between the two groups (early and late types) is the presence or not of recent star formation. In fact, the scenario of late-types turning into early-types is much more likely to happen than the contrary (Dressler et al., 1997, Fasano et al., 2000).

A more modern view about galaxy classification is the color-magnitude diagram. There is a bimodal distribution in the number of galaxies in such a diagram (Bell

et al., 2003, Gavazzi et al., 2010, Kaviraj et al., 2008), the so-called blue cloud and red sequence, and the region between them is the green valley. The galaxies of the red sequence are generally ellipticals, and the ones in the blue cloud are, typically, spirals. The ones in the green valley are galaxies transitioning between the two more prominent groups. Since luminosity scales somehow with mass, the spread in the absolute magnitude reflects a spread in galaxy mass too. Figure 1.4 shows a galaxy color-magnitude diagram from (Gavazzi et al., 2010).

The distribution of the different morphologies along the universe is not uniform but is strongly related with the environment in which the galaxy resides. The majority of them live in groups and clusters, while a smaller portion is found isolated in the field. Galaxies in dense environments, especially groups, are much more susceptible to interact with neighbors or with the intracluster gas, both gravitationally and hydrodynamically, and then undergo processes that can enhance or quench their star formation. The morphology-density relation shows that hat early-types dominate those dense environments, while the isolated galaxies are generally late-types (Dressler, 1980).

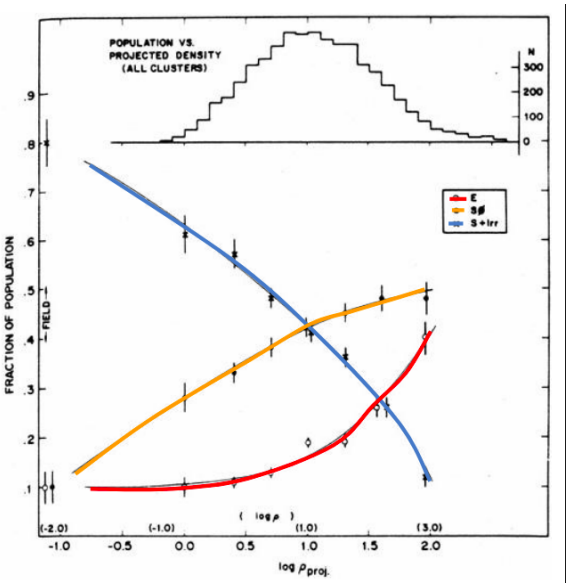

Figure 1.5: Morphology-density relation from (Dressler, 1980). As the density grows, the fraction of late-types decreases and the fraction of early-types increases. The curves were colored for better visualization.

Hereafter we present some of the main interaction mechanisms of interaction responsible for changes in the morphology and star formation in galaxies.

1.1.1 Galaxy-galaxy interaction

The interaction between galaxies can occur at any place but it is more common in dense environments because of the more significant number of those objects and the shorter distances between them (Mo et al., 2010).

Figure 1.6: Major merger occurring with the galactic duo UGC 2369. Credit: NASA / ESA / Hubble / A. Evans

Mergers

A merger is a fusion of galaxies when they collide. It is typically divided into major mergers, when the galaxies involved have similar masses, and minor mergers, when a smaller galaxy is captured by a much greater one (Lambas et al., 2012).

The minor merger does not modify the larger galaxy very much. Still, it can trigger the star formation in it due to the new amounts of gas absorbed (Bournaud et al., 2007), besides gradually enlarging the mass of the galaxy by the eventual absorption of other smaller ones. The major merger results in a galaxy very different from its progenitors, becoming an early-type in the end by removing the ISM by feedback processes (Bekki, 1998, Schombert, 1987, Toomre, 1977), but it can also trigger starbursts (Carroll & Ostlie, 2017) and nuclear activity (Hewlett et al., 2017).

Mergers can also be subdivided into types regarding the amount of gas in the galaxies involved. A fusion of two gas-rich galaxies produces a wet merger, increasing the star formation and can trigger quasar activity. A fusion of two gas-poor is the dry merger, that does not play an important roll in star formation but can increase the stellar mass. And there is still a mixed merger, which is a combination of a blue and a red galaxy (Lin et al., 2010).

Figure 1.7: Long tidal tail in the tadpole galaxy. Credit: NASA / ESA / Hubble / H. Ford, G. Illingworth, M. Clampin, G. Hartig

Tidal interactions

A slower gravitational interaction is provided by tidal forces, which can remove interstellar material and stars from the galaxy in the form of tidal tails. Approximately 10% of the galaxy's star formation takes place in the tails, and they can turn into compact stellar systems and dwarf galaxies (Vulcani et al., 2017, Mullan et al., 2010, Alavi & Razmi, 2015). This tidal interaction can occur with the cluster's gravitational potential, and in this case it is called strangulation.

Harassment

The harassment is an intense interaction that involves high-speed "fly-bys", i.e., when galaxies collide or pass too close to each other, but at high speed and in short time intervals. The galaxies do not merge, but this process can drastically modify the objects' morphology, quench the star formation, and even form rings of stars and gas around the galaxies (Moore et al., 1996).

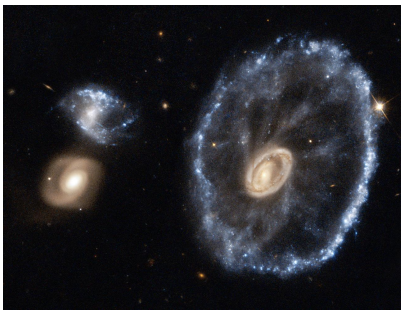

Figure 1.8: The Cartwheel galaxy, that has been recently harassed. The ring probably formed after one of the two minor galaxies passed through it and removed its disk's material. Credit: NASA / ESA / Hubble.

1.1.2 Galaxy-ICM interaction

Galaxies do not compose all the baryonic matter of groups and clusters. Those are also filled with a component of diffuse light and stellar clusters and hot gas of temperature between 10^7–10^8 K and typical density $\sim 10^{-27}\,\mathrm{gcm}^{-3}$ (Mo et al., 2010), known as intracluster medium (ICM). This gas is hotter than the interstellar medium (ISM) of the galaxy, which has a typical temperature between 10^3–10^4K, and the interaction between the two can change the temperature or the amount of the ISM. Since the star formation is linked with the efficiency with which the cold gas is converted into stars, such changes may alter the galaxy's star formation history (SFH).

Ram-pressure stripping

Galaxies falling in a dense environment will experience a ram-pressure due to their movement inside the ICM. The pressure is sensed by the satellite galaxies that orbit the center of the cluster's potential and the biggest cluster galaxy (BCG). In the case of a disk galaxy moving through the ICM face-on (velocity perpendicular to the plane of the disk), the ram-pressure can be computed as

$$P_{ram} = \rho v^2 \tag{1.1}$$

(Gunn & Gott, 1972), where ρ is the ICM density and v is the velocity of the satellite with respect to the cluster. If this ram-pressure is enough to surpass the galaxy's gravitational potential, it can remove the ISM, causing the ram-pressure stripping (RPS). The removal of interstellar gas can eventually quench the star formation and

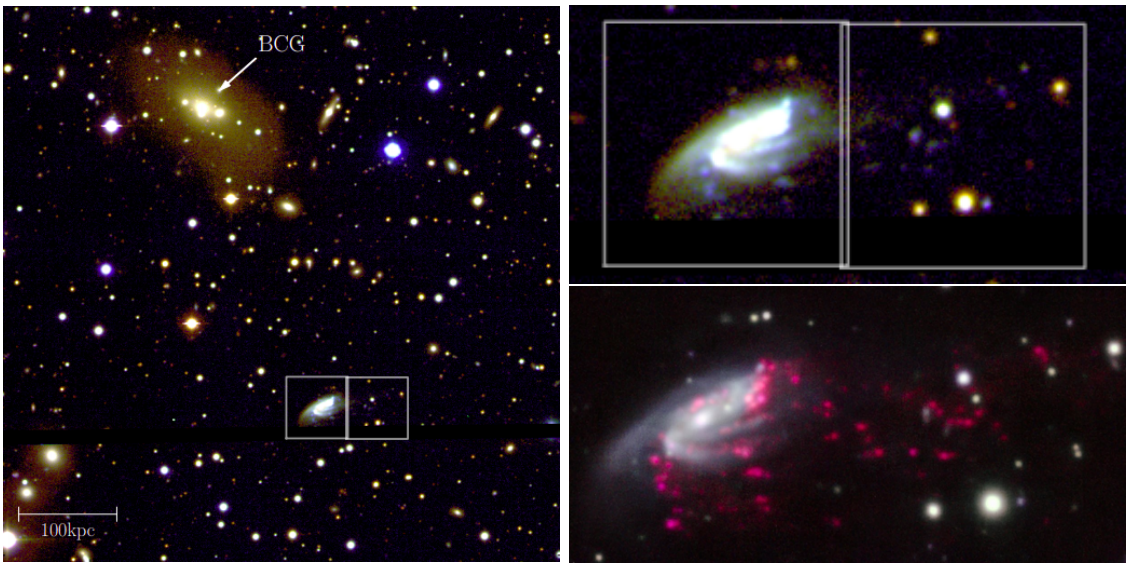

Figure 1.9: Left: RGB image of the central region of the cluster IIZW108, with the forming biggest cluster galaxy (BCG) and the jellyfish galaxy JO206 highlighted. Upper right: The same image zoomed on JO206. Bottom right: Image of JO206 along with the H_α emission in pink (Poggianti et al., 2017b).

may be one of the mechanisms responsible for turning late-types into early-types (Larson et al., 1980). RPS is more likely to occur with spirals but has also been observed in ellipticals, dwarfs and even ring galaxies (Kenney & Koopmann, 1999, 1997, Boselli et al., 2016, Fossati et al., 2018, Sheen et al., 2017, Kenney et al., 2014, Moretti et al., 2018). The most extreme cases of RPS create the jellyfish galaxies, which is the focus of this thesis.

1.2 Jellyfish galaxies

Jellyfish galaxies are the most extreme cases of galaxies undergoing ram-pressure stripping, called this way because of their resemblance with the aquatic living beings. The RPS produces gas tails in these galaxies, forming a unilateral asymmetry. In such tails there are lots of star-forming regions in such tails, which makes them visible in star formation excited emission lines, such as H_α ($\lambda = 6562.8\,\text{Å}$). Figure 1.9 shows an example of a jellyfish galaxy from (Poggianti et al., 2017b).

Various HII clumps form in the disk and the tail during such process, with similar $M_\star$–M_{gas}, $L_{H\alpha}$–σ and SFR–M_{gas} scaling relations (where $M_\star$ is the stellar mass, M_{gas} is the gas mass, $L_{H\alpha}$ is the H_α luminosity, σ is the dispersion velocity of the gas, and SFR is the star formation rate). A study of more than 500 clumps in the tails of 16 jellyfish galaxies revealed that they have median values of H_α

luminosity $L_{H\alpha} = 4 \times 10^{38}\, erg/s$, dust extinction $A_V = 0.5\, mag$, star formation rate $SFR = 0.003\, M_\odot/yr$, ionized gas density $n_e = 52\, cm^{-3}$, ionized gas mass $M_{gas} = 4 \times 10^4\, M_\odot$ and stellar mass $M_\star = 3 \times 10^6\, M_\odot$ (Poggianti et al., 2019). The stellar masses of the clumps are comparable to Ultra-Compact Dwarf (UCD) galaxies and Globular Clusters (GC), which rises the hypothesis that the tail clumps could originate part of the abundant population of such objects present in clusters (Hilker et al., 1999, Drinkwater et al., 2000, Wittmann et al., 2016).

This RPS phenomenon is greatly dependent on the satellite's velocity, its position in the cluster because ρ is a function of position, and the mass of both galaxy and cluster. The stripping is more efficient in high mass clusters and low mass galaxies ($M_\star < 10^9\, M_\odot$), but the most extreme cases are massive galaxies, because they have more gas available to be stripped (Jaffé et al., 2018). The jellyfish galaxies tend to be in central and intermediate regions of the clusters, with high velocities and preferentially on radial orbits, and probably entered the cluster between 1 and 3 Gyr ago (Jaffé et al., 2018, Yun et al., 2018). However, in the case of A901/2 multicluster system, which is a fusion of four clusters, the jellyfish galaxies are preferentially located near a boundary inside each subcluster where diffuse gas moving along with the subcluster and diffuse gas from the remnant of the system meet, due to the great change in velocity at those boundaries and a consequent increase in ram-pressure by a factor up to ∼1000 (Ruggiero et al., 2019, Roman-Oliveira et al., 2021).

Because of the nature of RPS, given that the gravitational bound of a galaxy decreases with radius, and as studies of jellyfish galaxies moving with striped tails in the line of sight (Bellhouse et al., 2017, 2019), it is believed that the stripping occurs in an outside-in scenario, i.e., the gas in the outskirts of the galaxies is removed first and then the gas of inner regions. There are a few cases of post-stripping galaxies observed, which have star formation in the central region but a truncated gas disk smaller than the stellar disk (Jaffé et al., 2018, Fritz et al., 2017).

Although these galaxies may end as early-types, the RPS is responsible for a global star formation rate (SFR) enhancement (Vulcani et al., 2018, Roman-Oliveira et al., 2019), likely due to shock waves produced by the ram-pressure (Vulcani et al., 2020). The SFR depends on various parameters of jellyfish galaxies and host clusters, but Gullieuszik et al. (2020) found some general trends: (i) galaxies with lower SFR in the tails are found at relatively large clustercentric distances; (ii) galaxies with large SFR in the tails (> 0.25 $M_\odot$ yr^{-1}) that are moving at great speed in the innermost regions of the clusters are massive and hosted in low-mass clusters; (iii) and the RPS occurs preferentially at intermediate clustercentric distances in massive

clusters and at lower distances in intermediate and low-mass clusters. Also, some cases of stripping galaxies were revealed to have much more significant amounts of molecular hydrogen than undisturbed galaxies and suggest that the stripping causes an efficient conversion of HI into H_2, what can be one cause of the enhanced star formation (Moretti et al., 2020a,b).

There is a discussion about RPS being able to trigger nuclear activity, although it is still unclear. A study of seven massive jellyfish galaxies ($4 \times 10^{10} \lesssim M_\star \lesssim 3 \times 10^{11} M_\odot$) with tails more extended than the disk diameter found that six of them host an AGN (Poggianti et al., 2017a, Radovich et al., 2019). Another theme in discussion is the magnetism in such objects. Müller et al. (2021) analyzed one case of a highly stripped galaxy. They found strong magnetic fields parallel to the direction of the tail, which may be a key factor in allowing in situ star formation in the tails, preventing the cold gas clouds from exchanging heat and momentum with their surroundings. In the thermal aspect, the stripped galaxies seem to present an extended X-ray emission component that follows the ISM spatially and is compatible with the thermal cooling of a warm plasma originated by the ICM-ISM interaction in the surface of the ISM (Campitiello et al., 2021). This interaction could cause the cooling and accretion of the ICM onto the galaxy, serving as fuel to star formation.

Franchetto et al. (2020) found that jellyfish galaxies with masses $10^{9.25} \leq M_\star \leq 10^{11.5} M_\odot$ have similar mass-metallicity relation to other cluster star-forming galaxies, suggesting that such relation is independent of RPS. However, it is above the expected by undisturbed galaxies for lower masses and involves a more complex scenario. One feature that differs between the two groups is the luminosity profile, which is less concentrated (lower Sérsic index) in stripped galaxies than other star-forming galaxies (Roman-Oliveira et al., 2021).

Such objects were observed for the first time in 1984 (Haynes et al., 1984), but only in the last decade they have been the aim of large surveys. Recently, 73 jellyfish candidates were identified in the multi-cluster system A901/2 (Roman-Oliveira et al., 2019, 2021). Based on such a sample Ruggiero et al. (2019) proposed that cluster mergers enhance the RPS and the formation of jellyfish galaxies. Other candidates were found in various systems at redshifts $0.04 < z < 0.07$ by the survey Wings (Poggianti et al., 2016a). From that, 94 were followed up by the GAs Stripping Phenomena in galaxies with MUSE (GASP) survey (Poggianti et al., 2017b), which observed them using an integral field spectrograph (IFS). This program provided the public data used in this work, and hereafter we explain the survey in more detail.

1.3 Data

In this section we present information and explanations about the data used in this work.

1.3.1 Integral field spectroscopy

Integral field units (IFU) instruments combine spectroscopy and imaging to obtain spatially resolved spectra of fields of the sky. For example, a standard photometric image has a pixel with a single value of luminosity. Instead, the IFUs give us a spectral distribution energy (SED) and each of the spectra is called "spaxel". This kind of data is organized as datacubes, 3-dimensional data where there are the two directions of the plane of the sky and an additional direction which is the wavelength of the emission detected.

Figure 1.10: Representative illustration of a datacube. Credit: Marc White (RSSA-ANU).

1.3.2 GASP

GAs Stripping Phenomena in galaxies with MUSE (GASP) is a program that observed 94 jellyfish galaxies at redshifts $0.4 < z < 0.7$, selected from the catalogue of jellyfish candidates (Poggianti et al. (2016b), P16) from WINGS and OmegaWINGS surveys (Poggianti et al., 2016a), which are a wide-field multi-wavelength survey of 76 clusters at low redshift, and 20 control field galaxies from Padova Millennium Galaxy and Group Catalogue (Calvi et al. (2011), PM2GC), using the IFS MUSE. The field of view (FoV) of 1 arcmin^2 is such that long distances from the disks of the galaxies are observed, which is necessary to completely encompass the tails completely. This survey was the first to observe a large sample of jellyfish candidates and is the biggest one until this day.

1.3.3 MUSE

The Multi-Unit Spectroscopic Explorer (Bacon et al. (2010), MUSE), is an IFU instrument located on the Very Large Telescope (VLT), in Chile. Its observations cover

the wavelength range of 4650 – 9300 Å (which encompasses the visible region of the spectrum and part of the NIR) with a spectral sampling of 1.25 Å, spectral resolution around 2.6 Å, FoV of 1 arcmin^2, angular sampling of 0.2 arcsec, and spatial resolution of 0.4 arcsec.

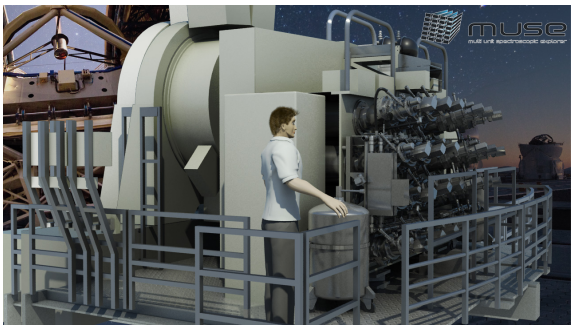

Figure 1.11: Representative illustration of the MUSE instrument. Source: `https://www.eso.org/sci/facilities/develop/instruments/muse.html`

MUSE's IFUs work with slicers, mirrors that separate the light into slices, both in the horizontal and vertical axis, and analyze each with different CCDs. GASP's observations use MUSE; it was able to observe regions of the galaxies distant from the disk and yet with incredible resolution.

1.4 Motivation

RPS plays an unquestionably important role in galaxy evolution. For instance, jellyfish galaxies are in the middle of a transitioning process between morphologies and SFRs. To fully understand the history of galaxies in dense environments, detailed studies of these objects are necessary.

Even though there are studies on jellyfish galaxies that use spectroscopic data, none have applied stellar population synthesis to it with the additional constraint on nebular emission given by FADO (Fitting Analysis using Differential evolution Optimization - see section 2.1). Such extra constraint is important when dealing with star-forming galaxies, because the gas ionized by massive stars ($M > 10\,M_{\odot}$), which are present in young populations ($t < 20\,Myr$), produce a considerable contribution to the luminosity, and guarantee that the amount of young populations are sufficient to produce the computed nebular spectra, besides the fact that it reduces the age-metallicity degeneracy. Therefore, we intend to study the stellar populations of these curious objects, both globally and spatially resolved, and with a novel method in the area.

We hope to shed light on the understanding of the SFH of those galaxies and the dependency of their populations with other physical parameters, such as intensity of the stripping and position on phase space (clustercentric distance and velocity). Also, this work intends to be a self-consistent comparative for the results obtained

by the GASP group, since we are using the same data and are interested in similar questions.

This thesis is structured as follows. In chapter 2, we explain the methodology and main calculations uses in our research. Then, in chapter 3, we present the results obtained with our analysis in the form of a scientific article that is in preparation. Finally, in chapter 4 we provide a summary and the main conclusions of our work.

Chapter 2

Methods

This chapter briefly describes the physics underlying the techniques applied in our analysis and the motivations that led us to use each one of them.

2.1 Stellar population synthesis (SPS)

Galaxies are composed mainly of stars, gas, dust, and dark matter. It is logical that the evolution of these objects as a whole depends on the evolution of their components. For example, gas and dust condense to form stars, which in turn change gas properties, such as temperature, density, and chemical abundances. That said, the different components in a galaxy have a strongly co-related evolution. For this reason, strategies to study the history of the stars or the gas prove themselves necessary. In this work, we used a method known as stellar population synthesis to study the stellar populations of jellyfish galaxies.

The stellar population of a galaxy, i.e., the age and metallicity of the stars that form it, has a leading role in understanding its formation and subsequent history. Thus, the stellar population analysis enables the comprehension of the star formation as a function of time and the discovery of processes the galaxy went through. Furthermore, the method of stellar population synthesis makes it possible to measure the characteristics of the populations based on their spectra.

The SPS technique consists of combining model spectra from simple stellar populations (SSPs), that are populations of stars formed from a single cloud and consequently have the same age and metallicity, to reproduce the observed spectra (Walcher et al., 2011). In this way, we know which combination of SSPs is needed to emit the detected radiation. Then, applying it to integral field spectroscopic data, we get a spatially resolved stellar population synthesis and are able to measure val-

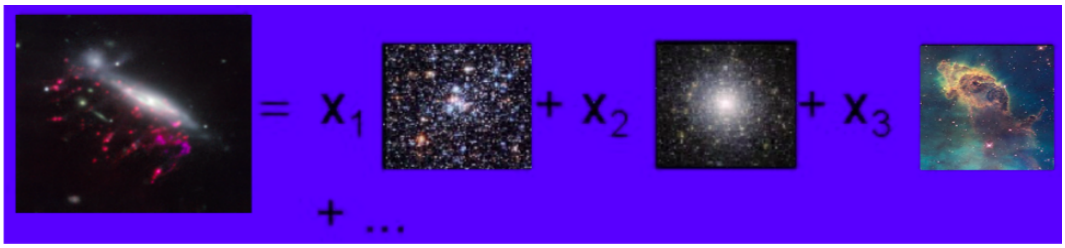

Figure 2.1: Illustrative representation of an SPS method. The population of the galaxy is described as a combination of different simple populations (plus the nebular emission, in the case of FADO code).

ues such as mean ages and metallicities and the fraction of each SSP in different regions of the galaxy.

2.1.1 Base of SSPs

To apply the synthesis technique, we need a base of model spectra of SSPs. In this work, we used a base of 138 simple stellar populations from Bruzual & Charlot (2003), with twenty-three (23) ages varying between 1 Myr and 13 Gyr and six (6) metallicities between 0.0001 and 0.05 (as shown in table 2.1). This base has a spectral resolution of 3.0 Å in the wavelength range encompassed by our data, a little poorer than MUSE's ∼2.6 Å resolution. Nevertheless, it has good spectral coverage of younger populations than other SSP models, down to 1Myr, which is very useful for synthesizing star-forming galaxies.

t (Gyr)	0.00100	0.00316	0.00501	0.00661	0.00871	0.01000	0.01445
	0.02512	0.04000	0.05500	0.10152	0.16090	0.28612	0.50880
	0.90479	1.27805	1.43400	2.50000	4.25000	6.25000	7.50000
	10.00000	13.00000					
Z	0.0001	0.0004	0.004	0.008	0.02	0.05	

Table 2.1: Ages and metallicities of the populations in the base.

2.1.2 Spectral Population Synthesis code FADO

One difficulty that exists in the SPS is how to deal with the age-metallicity degeneracy (Cardoso et al., 2019). It is well known that the more massive the star is, the shorter its life will be. As massive stars are hotter than lower mass ones, they irradiate more in the blue region of the visible spectrum. And if the low mass and red stars live longer, this means that the older the population is, the redder

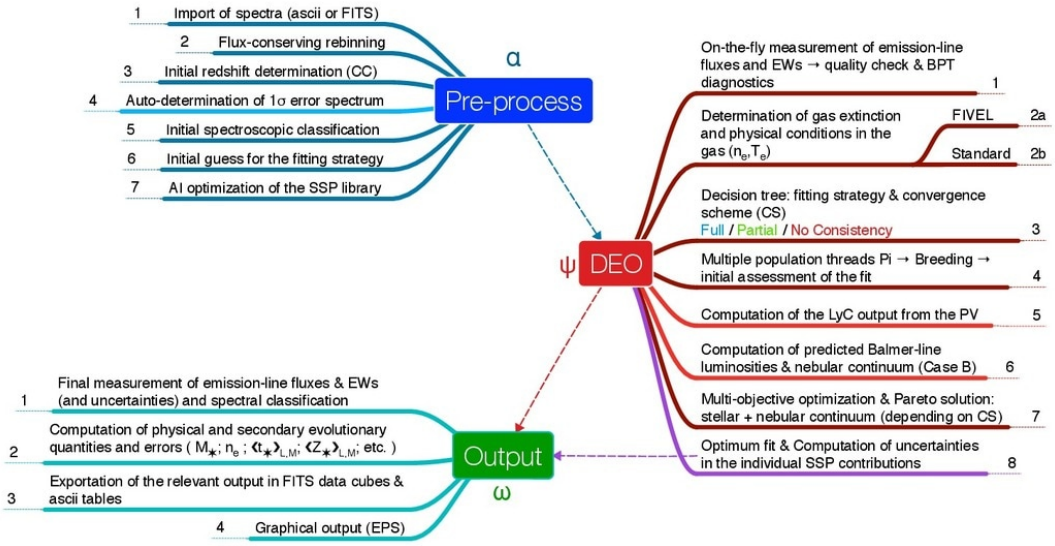

Figure 2.2: Scheme of FADO opperations (Gomes & Papaderos, 2017).

is its spectrum. But another thing that influences in the colors is the metallicity, as more metals mean more atoms with a bigger cross-section than H and He and, consequently, a growth of the radiative pressure. This causes the star to increase its radius and decrease its superficial temperature, becoming redder. In conclusion, populations of different ages and metallicities can produce similar SEDs.

There are several computer codes that propose different manners of performing the synthesis, but in this work, we have chosen to use FADO (Fitting Analysis using Differential evolution Optimization, Gomes & Papaderos, 2017), because it has an additional constraint compared to other existing synthesis codes that reduces the degeneracy and is also important when analyzing star-forming galaxies, such as jellyfish galaxies, that is the computation of the nebular emission. FADO synthesizes not only the stellar emission but also the emission of the ionized gas, which is measured using the flux of various emission lines (such as H, [NII], [SII] and [OIII]). Since hot and young stars (t $<$ 20 Myr) are responsible for the gas ionization, the code needs to make sure the results have the necessary amount of young stellar populations to produce the observed nebular emission characteristics. Figure 2.3 shows an example of a spectrum synthesized with FADO from Gomes & Papaderos (2017).

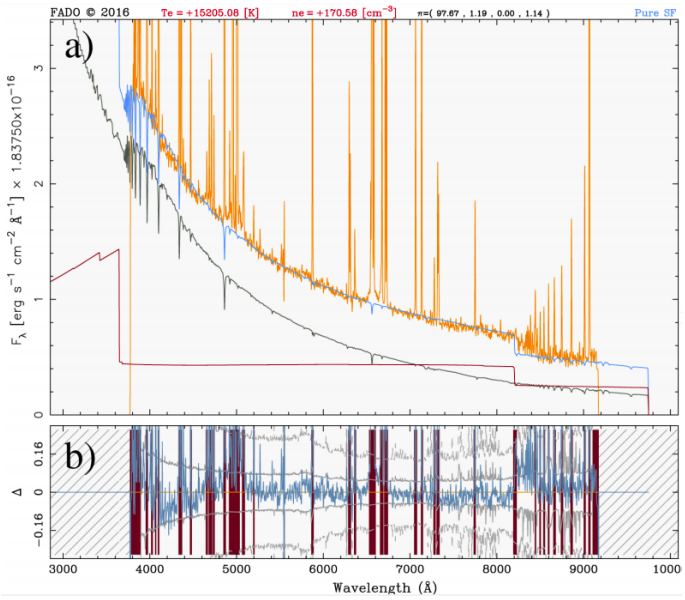

Figure 2.3: Example of a spectrum synthesized with FADO. **a)** The orange curve corresponds to the observed spectrum, in gray is the stellar emission, in red is the nebular emission, and in blue is the total (stellar+nebular) synthesized spectrum. **b)** The residuals of the synthesized spectra compared to the observed one (Gomes & Papaderos, 2017).

2.2 Interstellar extinction

The presence of dust in the interstellar medium (ice, hydrocarbons, silicates, and other molecules bigger than simple gases) is also responsible for reddening the spectrum of luminous objects. Those particles can scatter the light, and the scattering increases with frequency. That is, blue light is more scattered than red and the observed spectrum of stars is redder than the actual one. So it is important to correct the observed fluxes caused by this extinction. Figure 2.4 shows an illustration of such an effect.

The equation derived here actually returns an approximation of the actual attenuation, because they assume a volume of dust between the observer and the radioactive source. In the case of the nebular emission in the jellyfish galaxies, where the dust is mixed with the gas, the problem is more complex (see discussion in Calzetti et al., 2000). The following calculations are based on the Osterbrock & Ferland (2006) book.

The optical depth is defined as

$$\tau_\lambda = -\ln\left(\frac{I_{\lambda obs}}{I_{\lambda int}}\right), \tag{2.1}$$

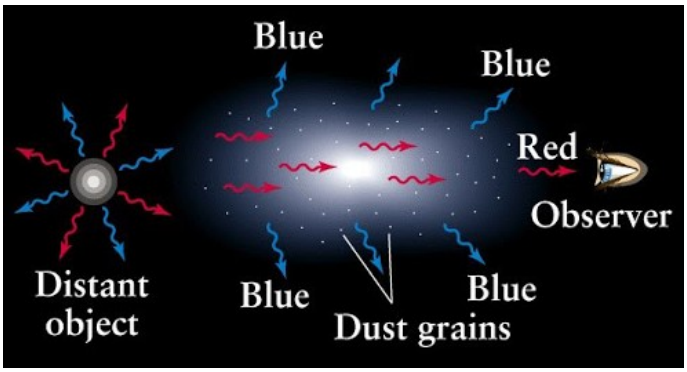

Figure 2.4: Illustration of the effect of dust in the scattering of the light of distant objects. Credit: Dmitri Pogosyan.

where $I_{\lambda int}$ is the intensity of the radiation intrinsic to the source in certain wavelength, and $I_{\lambda obs}$ is the observed intensity. Thus we have a relation between the observed intensities observed and intrinsic intensities of the spectral lines of those objects

$$\begin{aligned} I_{\lambda obs} &= I_{\lambda int} e^{-\tau_\lambda} \\ &= I_{\lambda int} 10^{-0.434\tau_\lambda}. \end{aligned} \tag{2.2}$$

We can write the extinction as $\tau_\lambda = Cf(\lambda)$, where C is the extinction coefficient, and $f(\lambda)$ is the extinction evaluated in the wavelength λ through a reddening law. In this work, we used the CCM law (Cardelli et al., 1988) to correct the spectra for the extinction due to dust from the Milky Way and the Calzetti attenuation law (Calzetti et al., 2000) for the extinction of the jellyfish galaxies. Thus we have

$$\begin{aligned} I_{\lambda obs} &= I_{\lambda int} 10^{-0.434Cf(\lambda)} \\ &= I_{\lambda int} 10^{-cf(\lambda)}. \end{aligned} \tag{2.3}$$

We can find c by taking the ratio between the intensity of two different spectral lines

$$\frac{I_{\lambda_1 obs}}{I_{\lambda_2 obs}} = \frac{I_{\lambda_1 int}}{I_{\lambda_2 int}} \times 10^{-c[f(\lambda_1)-f(\lambda_2)]}, \tag{2.4}$$

then

$$c = \frac{1}{f(\lambda_1) - f(\lambda_2)} \times \log\left[\left(\frac{I_{\lambda_1 int}}{I_{\lambda_2 int}}\right) \times \left(\frac{I_{\lambda_2 obs}}{I_{\lambda_1 obs}}\right)\right]. \tag{2.5}$$

We can also define the reddening in a wavelength as the magnitude difference

between the observed and the intrinsic intensities

$$A_\lambda = -2.5 \log \left(\frac{I_{\lambda obs}}{I_{\lambda int}} \right), \tag{2.6}$$

and comparing with equation 2.3, we have

$$\begin{aligned} 2.5cf(\lambda) &= A_\lambda \\ cf(\lambda) &= 0.4A_\lambda. \end{aligned} \tag{2.7}$$

Substituting $cf(\lambda)$ in equation 2.4 and using the definition $f(\lambda) = A_\lambda / A_V$, where A_V is the extinction at the central wavelength of the V band (5500Å), we get

$$\begin{aligned} \frac{I_{\lambda_1 obs}}{I_{\lambda_2 obs}} &= \frac{I_{\lambda_1 int}}{I_{\lambda_2 int}} \times 10^{-0.4[A_{\lambda_1} - A_{\lambda_2}]} \\ &= \frac{I_{\lambda_1 int}}{I_{\lambda_2 int}} \times 10^{-0.4 A_V [f(\lambda_1) - f(\lambda_2)]}. \end{aligned} \tag{2.8}$$

Then we can find A_V

$$A_V = \frac{2.5}{f(\lambda_1) - f(\lambda_2)} \times \log \left[\left(\frac{I_{\lambda_1 int}}{I_{\lambda_2 int}} \right) \times \left(\frac{I_{\lambda_2 obs}}{I_{\lambda_1 obs}} \right) \right]. \tag{2.9}$$

FADO performs those calculations using the hydrogen Balmer series lines. First, it computes the theoretical ratio $\frac{H_\alpha}{H_\beta}$ assuming case B recombination and the estimated electronic temperature and density come from the emission lines (e.g. [OIII] and [SII]). When it is impossible to evaluate one of these quantities, it is assumed either an electronic temperature $\mathrm{T}_e = 10^4\, K$, or electronic density $\mathrm{n}_e = 100\, cm^{-3}$. These two values give the ratio $\frac{H_\alpha}{H_\beta} = 2.86$, but different temperatures and densities do not change much the calculation.

2.3 Star formation rate

Star formation rate (SFR) is the mass of stars that are formed per year. One way to measure it is to calibrate it with the emission in some spectral line or photometric filter, based on models and simulations. In this work, we compute the SFR for the spaxels of the jellyfish galaxies using Kennicutt's relation (Kennicutt, 1998) for a (Chabrier, 2003) IMF, as done in Vulcani et al. (2018), Poggianti et al. (2019),

Gullieuszik et al. (2020):

$$SFR(M_{\odot}/yr) = 4.6 \times 10^{-42} L_{H\alpha}(erg/s)\,, \tag{2.10}$$

where $L_{H\alpha}$ is the luminosity of H_{α} corrected by nebular extinction, which was computed using the Calzetti reddening law (Calzetti et al., 2000). $L_{H\alpha}$ can be evaluated by $L_{H\alpha} = F_{H\alpha} 4\pi d^2$, where $F_{H\alpha}$ is the measured flux of H_{α} corrected by extinction and d is the distance to the galaxy.

2.4 Phase space

In dynamical system theory, a phase space is a space where all possible system states are represented. In a mechanical system, it turns out to be all possible values of momentum and positions it can assume. We can use this representation in Astronomy to study the dynamics of satellites on clusters and groups of galaxies.

Usually observational data allows us to measure just the projected values for distances and radial velocities, although we can obtain three-dimensional values from simulations. Also, we cannot know all possible states of a galaxy, but only its current position and velocity. So the use of phase space diagrams in extragalactic astrophysics is usually done by plotting the distribution of projected clustercentric distances and radial velocities of the satellites. Figure 2.5 shows an example of the phase space of jellyfish galaxies from Jaffé et al. (2018).

It is known from simulations that there is a sort of segregation in such diagrams based on the different orbits of the galaxies and how long they have entered the cluster. Recent infallers, intermediate infallers, which are backsplashing, and ancient infallers, which are virialized, tend to occupy distinct regions in the phase space (Rhee et al., 2017, Mahajan et al., 2011). As RPS is a mechanism dependant on the velocity of the jellyfish galaxies and the ICM density on its position, the galaxy position in the phase space is also related to its probability of being stripped and the intensity of the stripping (Jaffé et al., 2018, 2015).

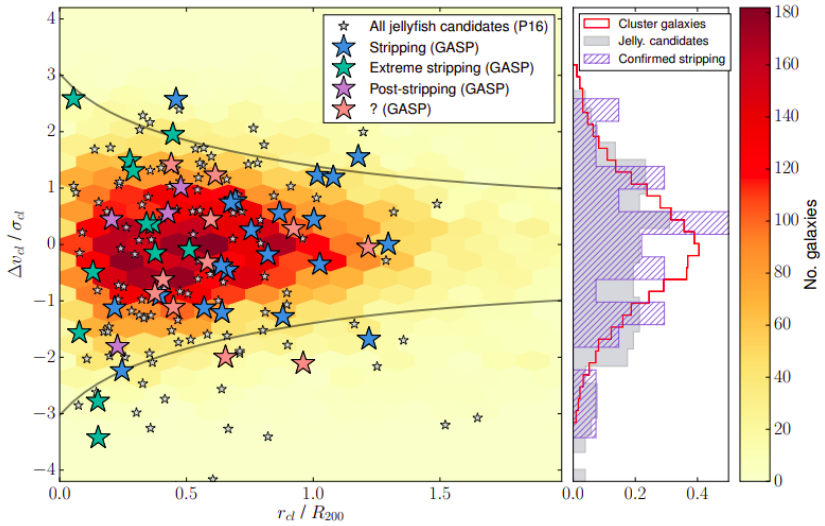

Figure 2.5: The location of projected position (r_{cl}) vs. velocity phase-space of all the jellyfish galaxy candidates from P16 (small gray stars) and the ones observed with MUSE by GASP so far (larger colored stars), separated by stripping stage as indicated. The background shows the distribution of all WINGS/OmegaWINGS clusters with spectroscopic completeness $> 50\%$ stacked together (orange color bar). The gray curve corresponds to the 3D escape velocity. To the right, a plot shows the velocity distribution of the overall cluster population of galaxies (open red histogram), all the jellyfish candidates from P16 (filled grey histogram), and the galaxies observed by GASP that are confirmed stripping cases (dashed blue histogram) at $r_{cl} < R_{100}$. All histograms have been normalized to unity for comparison (Jaffé et al., 2018).

Chapter 3

Results and Discussion

In this chapter, we present an early stage (most recent) draft version of a scientific article under preparation written about the subject of this work, which will be submited to Monthly Notices of the Royal Astronomical Society (MNRAS) as soon as the analysis is ready. Besides the content explored in detail in the last two chapters of this manuscript, this article also contains the results obtained and discusses these results.

MNRAS **000**, 1–7 (2021) Preprint 27 May 2021 Compiled using MNRAS LATEX style file v3.0

Self-consistent nebular emission and stellar population analysis of jellyfish galaxies through MUSE

Gabriel M. Azevedo[1] ⋆, Ana L. Chies-Santos[1], Rogerio Riffel[1], Augusto Lassen[1], et. al
[1]*Departamento de Astronomia, UFRGS, Av. Bento GonÃğalves, 9500, Porto Alegre, RS, Brazil*

Accepted XXX. Received YYY; in original form ZZZ

ABSTRACT
Jellyfish galaxies are curious objects undergoing extreme ram-pressure stripping. We present a spatially resolved stellar population analysis of 19 jellyfish candidates from the public ESO archive, having as an additional constraint the nebular emission, which is essential when dealing with star-forming galaxies. We obtain 2D morphological maps of mean stellar ages, mean stellar metallicities, and star formation rate surface densities for the galaxies, along with their individual star formation histories and a mean for the sample. We explore the relation between the mean stellar ages and metallicities with the stripping intensity and verify that the most disturbed stripped galaxies are on average younger than those with slight asymmetries in both ages weighted by mass and light. Also the galaxies with strong stripping are on average less metallic than the ones with intermediate stripping. The sample distribution in the phase space shows that the galaxies in the virialized region of the host clusters have light-weighted mean stellar ages typically above ∼ 2 Gyr and mass-weighted above ∼ 3 Gyr. In contrast, those in the recent infall area have mean stellar ages generally below such value. Also, the virialized region seems to have galaxies more metallic than the recent infallers, with light-weighted Z$\gtrsim$ 0.014 and mass-weighted Z$\gtrsim$ 0.016.

Key words: galaxies: clusters – galaxies: evolution: ram pressure stripping – galaxies: evolution: jellyfish galaxies – galaxies: star formation: star formation rate – spectrum: stellar population synthesis – spectrum: nebular emission

1 INTRODUCTION

Studying the different mechanisms through which galaxies transform is fundamental to understand galaxy formation and evolution theory thoroughly. Such complex objects exist in billions throughout all space-time, influencing and being influenced by the growth universe's large-scale structures.

One way to divide galaxies is by their color and star formation. There are three groups in this division: the red sequence, with red and generally quiescent galaxies; the blue cloud, with blue and usually star-forming galaxies; and the green valley, with galaxies in between the other two (Strateva et al. 2001; Hogg et al. 2002; Mateus et al. 2006; Baldry et al. 2004, 2006). The quiescent galaxies are commonly found in denser environments (Dressler 1980), like clusters and groups, with generally a massive early-type in the center orbited by satellite galaxies, both early and late-types. Thus, the environment has an essential role in modifying the morphology and the star formation in galaxies.

A phenomenon that changes both morphology and star formation in and around galaxies in dense environments is the ram pressure stripping (RPS) (Gunn & Gott 1972). This effect occurs when a galaxy falls into denser regions of the cluster/group and has its gas removed by the ram pressure caused by the gas from the intracluster medium when it is sufficient to overcome the gravitational potential of the galaxy. This stripping has already been observed in all sorts of galaxies: spirals (Kenney & Koopmann 1999; Fossati et al. 2018a; Poggianti et al. 2016b; Roman-Oliveira et al. 2019), ellipticals (Sheen et al. 2017), dwarfs (Kenney et al. 2014), and even ring galaxies (Moretti et al. 2018).

The most extreme cases of galaxies undergoing RPS are called jellyfish galaxies. They present structures similar to tails formed with the escaping gas and in the opposite direction of their movement in the cluster, making them look like the sea creatures. The jellyfish galaxies tend to be in central and intermediate regions of the clusters, with high velocities

⋆ gabriel.maciel.azevedo@gmail.com

and preferentially on radial orbits (Jaffé et al. 2018). The stripping is more efficient in high-mass clusters and low-mass galaxies, but the most extreme cases are massive galaxies. Both observations and simulations indicate that the jellyfish galaxies are recent infallers (Jaffé et al. 2018; Yun et al. 2018), with an infall time between ~ 1 and 3 Gyr. Those objects have been observed with photometry and spectroscopy in the visible region, ultraviolet, infrared, and radio (Jaffé et al. 2015; Poggianti et al. 2017; Fossati et al. 2018a; George et al. 2018; Roman-Oliveira et al. 2019), and both ionized, atomic and molecular gas were found in great amounts on the tails and discs of these objects (Deb et al. 2020; Ramatsoku et al. 2019, 2020; Moretti et al. 2020a; Roman-Oliveira et al. 2019; Poggianti et al. 2017; Fossati et al. 2018b; Jaffé et al. 2015; Poggianti et al. 2019).

The fate of these galaxies is not clearly understood yet. It is believed that the RPS can turn spirals and irregulars into S0's and ellipticals by removing the gas of the galaxy to the point of quenching it (Larson et al. 1980). Besides the transformation to S0s, spirals could suffer "diffusion" and maybe become dwarfs (Roman-Oliveira et al. 2021). However, during the process the star formation of the jellyfish galaxies is enhanced over all the galaxy (Vulcani et al. 2018), likely due to shock waves produced by the ram pressure (Vulcani et al. 2020). As a result, HII clumps are formed in the disc and the tails, extending up to 80 kpc from the galactic center. The clumps in both disk and tails follow similar M_{gas}–M_*, $L_{H\alpha}$–σ and SFR–M_{gas} relations (Poggianti et al. 2019), where $M_\star$ is the stellar mass, M_{gas} is the gas mass, $L_{H\alpha}$ is the H_α luminosity, σ is the dispersion velocity of the gas, and SFR is the star formation rate.

Studies of some jellyfish galaxies show that they have a much larger H_2 amount than undisturbed galaxies and suggest that the stripping causes the conversion of HI into H_2, which can be one cause for the enhanced star formation (Moretti et al. 2020a,b). Also, the stripped galaxies seem to present an extended X-ray emission component that follows the ISM and is compatible with the thermal cooling of a warm plasma. This evidence suggests that the ICM is being cooled in the surface of the ISM and can eventually be accreted and serve as fuel to star formation (Campitiello et al. 2021). Besides those aspects, a strong magnetic field parallel to the direction of the tails may be a critical factor in allowing in situ star formation in these tails, preventing the cold gas clouds from exchanging heat and momentum with their surroundings (Müller et al. 2021).

The SFR depends on various parameters of the galaxies and host clusters, but Gullieuszik et al. (2020) found some general trends: galaxies with lower SFR in the tails are found at relatively large clustercentric distances, galaxies with large SFR in the tails (> 0.25 $M_\odot$ yr^1) that are moving at great speed in the innermost regions of the clusters are massive and hosted in low-mass clusters, and the RPS occurs preferentially at intermediate clustercentric distances in massive clusters and at lower distances in intermediate and low-mass clusters.

Observations of a case of a jellyfish galaxy falling along the line of sight (Bellhouse et al. 2017; George et al. 2019) and the existence of truncated disks among jellyfish candidates (Fritz et al. 2017; Boselli et al. 2016) support the idea that the stripping is outside-in (i.e. occurs first in the outer regions of the galaxy). It has also been proposed that part of the great amount of ultra-compact dwarfs (UCD) and intracluster globular clusters (GC) at low redshift clusters can originate from those HII regions that are stripped from the tails of jellyfish galaxies (Poggianti et al. 2019).

The merging of clusters is one kind of system that may enhance the formation of jellyfish galaxies. For example, the multi-cluster system A901/2, formed by four subclusters, presents a large population of stripped galaxies, and they seem to be preferentially near boundary regions where diffuse gas moving along with the subcluster and diffuse gas from the remnant of the system meet (Ruggiero et al. 2019; Roman-Oliveira et al. 2019, 2021). In such regions, the significant change in the speed increases the ram pressure up to a factor of ~1000.

Although pieces of evidence of the tails of gas in such stripped galaxies were observed the first time in 1984 (Haynes et al. 1984), it was just in the last years that astronomers have been dedicating more special attention to those objects, creating large catalogs and commanding surveys specifically about the jellyfish galaxies. For instance, recently, 70 jellyfish candidates were identified in the system A901/2 (Roman-Oliveira et al. 2019). Another important sample is the one from Poggianti et al. (2016a), which consists in candidates at redshifts $0.04 < z < 0.07$. From those galaxies, 94 were further observed by the GAs Stripping Phenomena in galaxies with MUSE (GASP) survey (Poggianti et al. 2017), which is a spatially-resolved spectroscopic survey using the spectrograph MUSE in the very large telescope (VLT).

This study has performed stellar population synthesis (SPS) in public datacubes downloaded from the ESO archive and belonging to the GASP survey. The data and sample selection are explained in section 2, along with more details about the GASP sample. The codes used in this work are presented in section 3. In section 4, we show the results of the synthesis and the respective analyses. In section 5, we discuss the relation of the synthesis results with the environment and the intensity of the stripping. Finally, in section 6, we summarize what has been done in this work and our conclusions. Appendix A presents 2D morphology maps of mean stellar ages, mean stellar metallicities, H_alpha emission and surface density star formation rate for the galaxies of the sample.

Throughout this work, it was used the Chabrier (2003) initial mass function and the cosmological values: $H_0 = 67\,km\,s^{-1}Mpc^{-1}$, $\Omega_M = 0.3$, $\Omega_\Lambda = 0.7$ (Kozmanyan et al. 2019).

2 DATA

In this work, we make use of 19 of the public datacubes of galaxies from GASP (Poggianti et al. 2017) with enough signal-to-noise ratio (S/N). We first downloaded all the 94 datacubes of jellyfish galaxies from both data releases 1 and 2 from GASP. Most parts of the galaxies have very low S/N in the spectral continuum of the ionized gas tails. A value of S/N≥5 in the continuum is essential to guarantee minimum reliability to the results of stellar population synthesis (SPS) methods. To contour it, we have binned the spaxels 4 to 4 (sum 16 spaxels in 1), in order to improve the S/N of the whole sample, without losing too much spatial reso-

Table 1. Right ascension, declination, redshift, logarithm of stellar mass, and host cluster for the galaxies of our sample.

Galaxy	RA	Dec	z	log($M_\star/M_\odot$)	Cluster
JO10	00 57 41.59	-01 18 44.24	0.0469	10.76	A119
JO147	13 26 49.73	-31 23 44.79	0.0503	11.03	A3558
JO162	13 31 29.87	-33 03 18.56	0.0451	9.42	A3560
JO20	01 08 54.99	+02 14 20.92	0.1479	——	A147
JW108	06 00 47.94	-39 55 06.90	0.0475	10.48	A3376
JW56	13 27 03.03	-27 12 58.04	0.0453	9.05	A1736
JO138	12 56 58.49	-30 06 05.57	0.0570	9.65	A3532
JO119	06 29 59.08	-54 47 38.34	0.0493	——	A3395
JO27	01 10 48.50	-15 04 42.92	0.0493	9.50	A151
JO36	01 12 59.40	+15 35 29.59	0.0404	10.81	A160
JO49	01 14 43.92	+00 17 10.07	0.0447	10.68	A168
JO113	03 41 49.23	-53 24 12.16	0.0549	9.69	A3158
JO13	00 55 39.67	-00 52 35.47	0.0475	9.82	A119
JO159	13 26 35.74	-30 59 36.13	0.0477	9.82	A3558
JO160	13 29 28.58	-31 39 25.46	0.0481	10.06	A3558
JO194	23 57 00.74	-34 40 49.94	0.0418	11.18	A4059
JO135	12 57 04.32	-30 22 30.19	0.0540	10.99	A3530
JO190	22 26 53.67	-30 53 10.66	0.0130	——	A3880
JO85	23 24 31.41	+16 52 05.93	0.0351	10.67	A2589

lution (other S/N improvement methods were tried, such as Butterworth filtering and Voronoi binning, but they did not provide satisfactory results). Then we visually selected those galaxies whose most part of the tails had S/N ≥ 5 in the wavelength range 5540 – 5600Å, resulting in a final sample of 19 jellyfish candidates. We used the dust maps from Schlegel et al. (1998) and the CCM law with R_v = 3.1 (Cardelli et al. 1988; O'Donnell 1994) to correct the fluxes according to the extinction caused by the dust from the Milky Way.

GASP is a large program that observed galaxies undergoing extreme ram pressure stripping (Poggianti et al. 2017). The sample is composed of 94 jellyfish candidates and 20 control galaxies at 0.04 < z < 0.07. and was based on a catalog of selected jellyfish candidates from WINGS and OmegaWINGS surveys (Poggianti et al. 2016a), chosen by visual inspection. The control sample is formed by galaxies from Padova Millennium Galaxy and Group Catalogue (PM2GC) (Calvi et al. 2011).

The data was obtained using the Multi-Unit Spectroscopic Explorer (Muse) Bacon et al. (2010)) on the Very Large Telescope (VLT), covering the wavelength range of 4650 – 9300 Å with spectral sampling of 1.25 Å, FoV of 1 acrmin^2, angular sampling of 0.2 arcsec, and spatial resolution of 0.4 arcsec, so it is capable of observing regions of the galaxies distant from the disk and yet with incredible resolution. Figure 1 presents an image of the galaxy JO113, located at z=0.0549 in A3158 cluster, which has strong signatures of gas stripping, and Table 1 lists all the galaxies in the sample and some general information about them, taken from the Jellyfish galaxy candidates in galaxy clusters (Poggianti et al. 2016b) catalog and from Gullieuszik et al. (2020).

3 SPECTRAL POPULATION SYNTHESIS

To implement the SPS in our datacubes, we used the code FADO (Fitting Analysis using Differential evolution Optimization, Gomes & Papaderos 2017). FADO uses a genetic differential evolution optimization algorithm to fit the spectra, with the additional constraint of the nebular emission (continuum plus lines), computed with the flux of various emission lines (Hα, Hβ, [NII], [SII], [OIII], etc). This

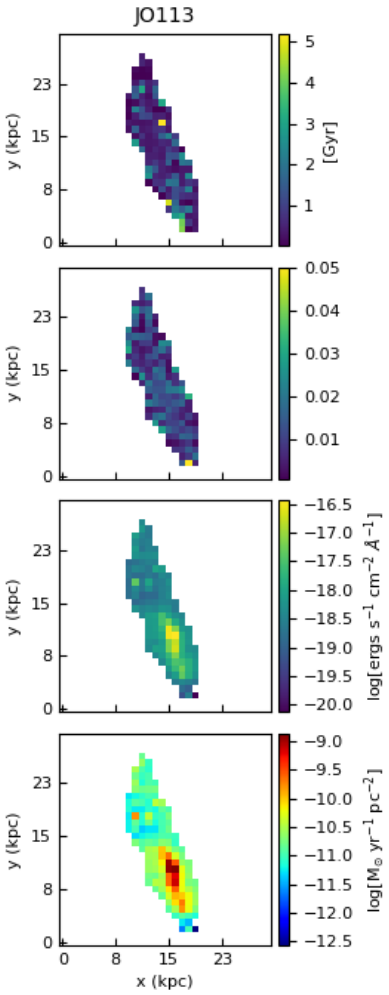

Figure 1. From top to bottom: maps of t_{light}, Z_{light}, logarithm of the flux of H_α, star formation rate surface density of the galaxy JO113, located at z=0.0549 in A3158 cluster.

constraint is extremely important when synthesizing star-forming galaxies (Cardoso et al. 2019) since it enables the computation of nebular spectra (in addition to the stellar one) and the amount of young stars (t < 20 Myr) necessary to produce the measured gas ionization. Thus, it is essential for analyzing the stars in the tails of the jellyfish galaxies and also in the disks, which present lots of HII regions. It is known that the star formation rate of these galaxies increases in all of its regions while suffering stripping (Vulcani et al. 2018), which means that in most of the cases, we have young stellar populations through all extensions of the jellyfish galaxies.

In this work it was used a base of 138 simple stellar population (SSP) from Bruzual & Charlot (2003), with 23 different ages varying between 1 Myr and 13 Gyr (t = 1.00, 3.16, 5.01, 6.61, 8.71, 10.00, 14.45, 25.12, 40.00, 55.00, 101.52, 160.90, 286.12, 508.80, 904.79 Myr and 1.27805, 1.434, 2.500, 4.250, 6.250, 7.500, 10.000, 13.000 Gyr) and 6 metallicities between 0.0001 and 0.05 (Z = 0.0001, 0.0004, 0.004, 0.008, 0.02 and 0.05). This base has a spectral resolution of 3.0 Å in the wavelength range encompassed by our data, a little poorer than MUSE's ~2.6 Å resolution, and have spectra of

younger populations compared to other SSP models, down to 1Myr, which is very useful for synthesizing star-forming galaxies.

4 STELLAR POPULATIONS

Performing SPS on datacubes allows us to analyze the observed objects spatially since we have one spectrum for each pixel, which corresponds to different regions in the field of view. For one given spectrum the synthesis computes the fraction of the light of that spectrum that originates from each SSP (e.g. 0.4 of the light is emitted by a population with age = 2 Gyr and Z = 0.2, and 0.6 is emitted by a population with age = 0.1 Gyr and Z = 0.01). We can convert the fraction of light to the fraction of mass by using luminosity-mass relations. In this work, we only performed the synthesis in the spectra with S/N $\geq$ 5, measured in the continuum window between 5540 Å and 5600 Å.

We then computed the mean stellar ages and metallicities of each spaxel using both the fractions of light (light-weighted) and the fraction of mass (mass-weighted). More massive stars are generally much more luminous but also much less numerous than less massive ones and also have a shorter lifetime. Therefore, the luminosity of a population is dominated by younger stars, and weighting the populations by light gives higher fraction of young populations. The mass, though, is dominated by the less massive stars because they are more numerous, and since they last much longer than the more massive ones, weighting the populations by mass typically gives higher fractions of older populations. Because of this difference, it is interesting to present our measures in both manners. Figure 1 presents 2D morphology maps of mean stellar ages and metallicities weighted by light and by mass for one of the galaxies studied in this work.

Here it is important to define the quantities mentioned above. For each spaxel, the mean stellar ages are defined in two ways (Fernandes et al. 2005; Gomes & Papaderos 2017): the first weighted by light

$$< t >_L = \sum_{j=1}^{N_\star} x_j t_j \,, \tag{1}$$

and the second weighted by mass

$$< t >_M = \sum_{j=1}^{N_\star} m_j t_j \,, \tag{2}$$

where t_j is the age of the jth SSP from the base, x_j is the fraction with which it contributes to light, m_j is the fraction with which it contributes to mass, and $N_\star$ is the number of SSPs in the base. Similarly, the mean stellar metallicities are defined as

$$< Z >_L = \sum_{j=1}^{N_\star} x_j Z_j \,, \tag{3}$$

and

$$< Z >_M = \sum_{j=1}^{N_\star} m_j Z_j \,, \tag{4}$$

where Z_j is the metallicity of the jth SSP.

From those mean stellar ages and metallicities for each spaxel, the mean stellar ages and metallicities of the whole galaxies are computed as

$$t_{light} = \frac{1}{N_S} \sum_{i=1}^{N_S} < t >_{Li} \,, \tag{5}$$

$$t_{mass} = \frac{1}{N_S} \sum_{i=1}^{N_S} < t >_{Mi} \,, \tag{6}$$

and as

$$Z_{light} = \frac{1}{N_S} \sum_{i=1}^{N_S} < Z >_{Li} \,, \tag{7}$$

$$Z_{mass} = \frac{1}{N_S} \sum_{i=1}^{N_S} < Z >_{Mi} \,, \tag{8}$$

where the index i represents the ith spaxel and N_S is the number of spaxels in the galaxy.

We also compute the star formation rate in each pixel by using Kennicutt's relation (Kennicutt 1998) for a Chabrier (2003) IMF, as done in Vulcani et al. (2018); Poggianti et al. (2019); Gullieuszik et al. (2020):

$$SFR(M_\odot/yr) = 4.6 \times 10^{-42} L_{H\alpha}(erg/s), \tag{9}$$

where $L_{H\alpha}$ is the luminosity of H_α corrected by nebular extinction, which is computed using the Calzetti reddening law. $L_{H\alpha}$ can be evaluated by $L_{H\alpha} = F_{H\alpha} 4\pi d^2$, where $F_{H\alpha}$ is the measured flux of H_α (corrected by extinction), and d is the distance to the galaxy, which was computed with Wright (2006) cosmology calculator. Such an equation gives us an "instantaneous" SFR since atomic hydrogen is ionized by hot and massive stars in populations with $\lesssim$ 20 Myr. Thus dividing the SFR values by the area of each spaxel in kpc^2 we obtained the star formation surface densities.

In order to analyze the distribution of the star formation through time, we plotted cumulative histograms of the fraction of stars formed in each of the ages of our base, separating light-weighted and mass-weighted results, for the 19 galaxies of the sample, as a way to see their star formation history (SFH). We also made a mean histogram of the entire sample. Table 1 presents the ages in which 50 percent, 70 percent, and 90 percent of the stars of each galaxy were already formed, and also the mean values. It is important to remember that such percentages are not measured in relation to the number of stars but are fractions of light or mass, and it is also good to remark that the age intervals were displaced in equal distances in Figure 2 for better visualization and do not follow a linear scale, so higher inclination in the curves does not necessarily imply greater SFR.

5 RESULTS AND DISCUSSION

Intending to explore the relation of stellar populations of the galaxies with the intensity of the stripping, we separated our sample with respect to the J-class, a visual classification of jellyfish candidates, with J5 being the most disturbed ones and J1 being those with slight asymmetries (Poggianti et al. 2016b). Figure 3 shows the t_{light} and t_{mass}, as well as Z_{light} and Z_{mass}, of each class. The mean stellar ages present a decreasing pattern, with J1 galaxies being typically older

Table 2. t_{light}, t_{mass}, and ages when 50 percent, 70 percent and 90 percent of the stars ware formed, for all the galaxies, as well as the mean values for the entire sample.

		Mass-weighted ages (Gyr)				Light-weighted ages (Gyr)			
Galaxy	J-class	Mean stellar age	Age 0.5 of stars formed	Age 0.7 of stars formed	Age 0.9 of stars formed	Mean stellar age	Age 0.5 of stars formed	Age 0.7 of stars formed	Age 0.9 of stars formed
JO10	1	7.29	7.5	1.434	0.904	3.79	1.434	0.904	0.014
JO147	1	9.21	13	6.25	1.278	3.39	1.278	0.101	0.04
JO162	1	4.79	4.25	0.904	0.286	2.3	0.904	0.286	0.005
JO20	1	9.03	10	4.25	2.5	4.93	2.5	1.278	0.005
JW108	1	8.57	10	6.25	0.508	3.56	0.904	0.286	0.006
JW56	1	4.42	0.286	0.055	0.005	0.61	0.005	0.003	0.003
JO138	2	3.81	1.278	0.904	0.286	1.63	0.508	0.286	0.014
JO119	3	4.96	1.434	0.904	0.286	1.82	0.904	0.286	0.008
JO27	3	2.88	0.904	0.286	0.055	1.13	0.286	0.101	0.01
JO36	3	6.92	6.25	1.278	0.904	2.89	0.904	0.904	0.005
JO49	3	4.29	2.5	0.904	0.904	2.37	0.904	0.904	0.008
JO113	4	2.77	0.904	0.286	0.04	0.93	0.286	0.055	0.006
JO13	4	4.53	2.5	0.904	0.055	2.04	0.508	0.16	0.005
JO159	4	1.45	0.508	0.286	0.16	0.62	0.286	0.286	0.006
JO160	4	5.15	4.25	0.904	0.508	1.87	0.904	0.508	0.01
JO194	4	6.22	4.25	1.434	0.508	2.91	1.278	0.286	0.008
JO135	4	7.79	10	2.5	0.904	3.61	1.278	0.508	0.04
JO190	5	1.06	0.286	0.01	0.005	0.46	0.014	0.01	0.003
JO85	5	4.16	1.434	0.904	0.286	1.72	0.904	0.16	0.01
ENTIRE SAMPLE		5.24	2.5	0.904	0.16	2.24	0.904	0.286	0.005

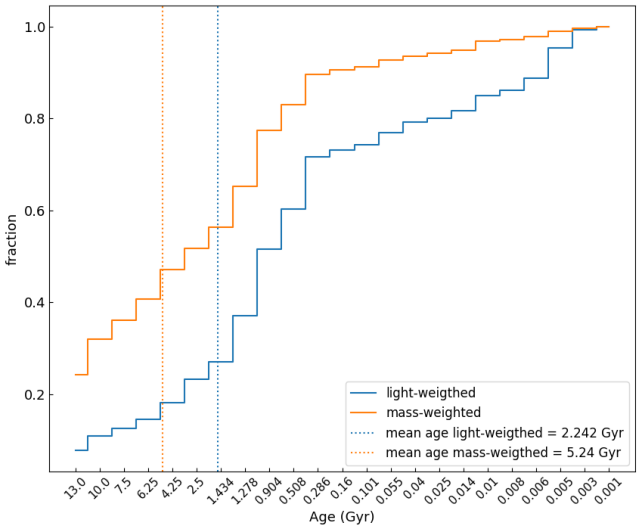

Figure 2. Mean cumulative histogram for the fraction of stars formed along the history of the galaxies.

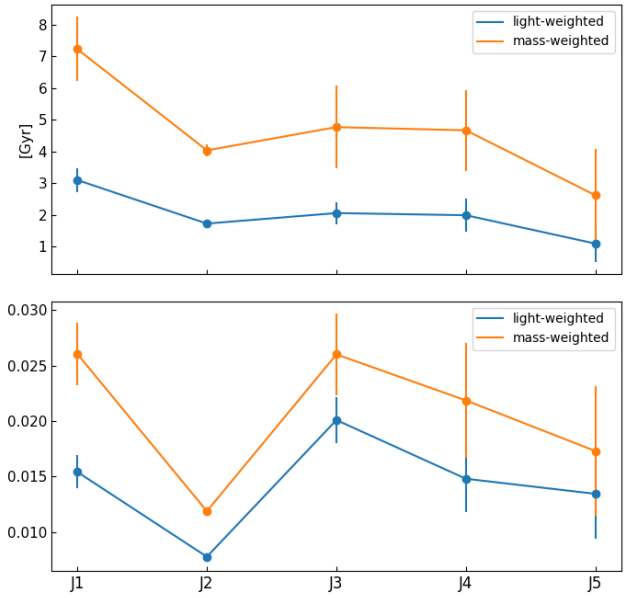

Figure 3. Top pannel: mean stellar ages grouped by J-class. Bottom pannel: mean stellar metallicities. J5 represents the group of the most stripped jellyfish candidates, while J1 represents those galaxies with slight asymmetries.

than the others and J5 ones being generally younger. This may be because J5 is the galaxies with the most extended tails, and their SFR is larger.

The metallicity also presents a clear decrease from J3 to J5, although the same cannot be said of the range from J1 to J3. The most dissonant point in both ages and metallicities is the one corresponding to J2 class. It is important to notice that only one galaxy of our sample belongs to this group, so the plot does not show the mean stellar age and metallicity of a group of J2 galaxies, but actually the measurements for a single galaxy. Our ample is formed of six J1, one J2, four J3, six J4 and two J5, and the classes of each jellyfish candidate are presented in Table 2.

It is worth remarking that the error bars in figure 3 are uncertainties in the mean and do not represent the actual spread of the galaxy mean stellar ages, which is larger. For example, the J1 galaxies have mean stellar ages 4.5 Gyr $\lesssim t_{light} \lesssim$ 9 Gyr and 0.6 Gyr $\lesssim t_{mass} \lesssim$ 3.5 Gyr. Since our sample contains just 1 J2 galaxy and 2 J5s, it is needed to verify if larger samples follow the same patterns found here.

The mean stellar age for one galaxy was calculated as the arithmetic average of the mean stellar ages of each spaxel, and the mean stellar age of the J-classes as the arithmetic mean of the ages of jellyfish candidates in each group. The errors were propagated using

$$\sigma_{gal} = \sqrt{\sigma_1^2 + \sigma_2^2 + \sigma_3^2 + ...} \quad (10)$$

where σ_{gal} is the uncertainty in the galaxy's mean stellar age and σ_i is the uncertainty in the mean stellar age of each spaxel. Similarly, we compute the error in the mean stellar age of a class using σ_i as the mean stellar ages of the jellyfish galaxies.

Another analysis we made is exploring a phase space diagram, which is a plot of the galaxy line-of-sight velocity normalized by the cluster velocity dispersion vs the projected clustercentric distance normalized by the R_{200}. Those values for the galaxies of our sample were taken from Gullieuszik et al. (2020), although three of them (JO190, JO119, and JO20) do not have such information presented. Figure

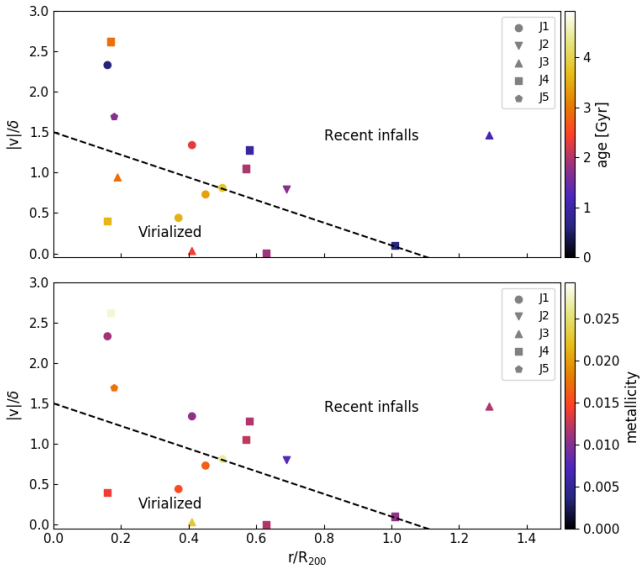

Figure 4. Phase space diagram of our sample, presenting the radial velocity vs clustercentric distance, color-coded by t_{light} (top pannel) and by Z_{light} (bottom pannel). The triangle represents the approximated region where one expects most galaxies to be virialized.

4 shows two of those diagrams, where t_{light} and Z_{mass} are plotted in the color dimension. The triangle in the lower-left corner is the approximate region where one expects that most galaxies are virialized (Mahajan et al. 2011; Jaffé et al. 2015, 2018). The region outside the triangle and to the left is the region of recent infallers, where most galaxies are in their first infall or in the "back-splash" (i.e. previously entered the cluster but are now beyond the virial radius). This segregation is based on the time since infall (which is defined as the time since the galaxy crossed R_{200} for the first time) and the virialized region is dominated by galaxies that entered the cluster $\gtrsim$ 4 Gyr, while the outside of the triangle is dominated by the ones that entered $\lesssim$ 3Gyr (Rhee et al. 2017).

It is visible that all jellyfish candidates in the virialized region have in general older populations ($t_{light} \gtrsim$ 2 Gyr and $t_{mass} \gtrsim$ 3 Gyr) than the ones in the region of recent infall. This could be explained by the virialization itself. The virialized galaxies have spent more time evolving in the environment, being probably almost completely stripped and becoming more stable. Similar segregation is also seen in the metallicity. The galaxies in the virialized region are typically more metal-rich ($Z_{light} \gtrsim 0.014$ and $Z_{mass} \gtrsim 0.016$) than the others. For comparison, the solar metallicity is adopted as $Z_{\odot}$ =0.02 in the models used in Chabrier (2003).

6 SUMMARY AND CONCLUSIONS

In order to perform spatially resolved stellar population synthesis in jellyfish galaxies, we first selected a sample of objects with good continuum S/N from GASP, which consists of integral field spectroscopic data. Our final sample composed of 19 galaxies with different intensities of stripping. We implemented the synthesis on the data using the code FADO with a base of 138 SSPs from (Bruzual & Charlot 2003).

FADO allows us to synthesize spectra under self-consistent boundary conditions based on measurements of emission lines and computation of nebular emission, resulting in more reliable results for star-forming regions, which involve ionizing populations (t $\lesssim$ 20 Myr). Applying it to every spaxel of our datacubes, we created maps of mean stellar ages and metallicities, H_{α} emission, and SFR surface densities.

We made cumulative histograms with the fraction of light/stellar mass formed at each age of the basis for the galaxies, along with a mean histogram of the entire sample to see a general behavior of SFHs. Those were translated into a table showing the mean stellar ages and the basis ages when 50, 70, and 90 percent of the stars had been formed.

Grouping the jellyfish candidates of the sample based on their J-class, which is a visual classification that represents the intensity of the stripping, going from 1 (weaker) to 5 (stronger), we note a clear decrease of mean stellar ages with increasing class, although the spread of ages in each group is quite large. A decrease of mean stellar metallicity is also noticeable from J3 to J5, but those values for J1 are similar or lower than for J3. Notice that we have only one J2 and two J5 galaxies in the sample, which gives us poor statistics, and such results must be verified with larger samples.

The phase space diagram, which is the radial velocity versus the clustercentric distance of the galaxies, shows that jellyfish galaxies in the virialized region of the diagram are typically older then the ones in the region of recent infall, with ages $t_{light} \gtrsim$ 2 Gyr and $t_{mass} \gtrsim$ 3 Gyr. Also the virialized region seems to have galaxies more metal-rich than the recent infallers, with $Z_{light} \gtrsim 0.014$ and $Z_{mass} \gtrsim 0.016$.

ACKNOWLEDGEMENTS

REFERENCES

Bacon R., et al., 2010, in McLean I. S., Ramsay S. K., Takami H., eds, Society of Photo-Optical Instrumentation Engineers (SPIE) Conference Series Vol. 7735, Ground-based and Airborne Instrumentation for Astronomy III. p. 773508, doi:10.1117/12.856027

Baldry I. K., Balogh M. L., Bower R., Glazebrook K., Nichol R. C., 2004, in Allen R. E., Nanopoulos D. V., Pope C. N., eds, American Institute of Physics Conference Series Vol. 743, The New Cosmology: Conference on Strings and Cosmology. pp 106–119 (arXiv:astro-ph/0410603), doi:10.1063/1.1848322

Baldry I. K., Balogh M. L., Bower R. G., Glazebrook K., Nichol R. C., Bamford S. P., Budavari T., 2006, MNRAS, 373, 469

Bellhouse C., et al., 2017, ApJ, 844, 49

Boselli A., et al., 2016, A&A, 587, A68

Bruzual G., Charlot S., 2003, MNRAS, 344, 1000

Calvi R., Poggianti B. M., Vulcani B., 2011, MNRAS, 416, 727

Campitiello M. G., et al., 2021, ApJ, 911, 144

Cardelli J. A., Clayton G. C., Mathis J. S., 1988, ApJ, 329, L33

Cardoso L. S. M., Gomes J. M., Papaderos P., 2019, A&A, 622, A56

Chabrier G., 2003, PASP, 115, 763

Deb T., et al., 2020, MNRAS, 494, 5029

Dressler A., 1980, ApJ, 236, 351

Fernandes R. C., Mateus A., SodrÃl' L., StasiÅĎska G., Gomes J. M., 2005, Monthly Notices of the Royal Astronomical Society, 358, 363

Fossati M., et al., 2018a, A&A, 614, A57
Fossati M., et al., 2018b, A&A, 614, A57
Fritz J., et al., 2017, ApJ, 848, 132
George K., et al., 2018, MNRAS, 479, 4126
George K., et al., 2019, MNRAS, p. 1383
Gomes J. M., Papaderos P., 2017, A&A, 603, A63
Gullieuszik M., et al., 2020, ApJ, 899, 13
Gunn J. E., Gott J. Richard I., 1972, ApJ, 176, 1
Haynes M. P., Giovanelli R., Chincarini G. L., 1984, ARA&A, 22, 445
Hogg D. W., Blanton M. R., Eisenstein D. J., 2002, in American Astronomical Society Meeting Abstracts. p. 148.04
Jaffé Y. L., Smith R., Candlish G. N., Poggianti B. M., Sheen Y.-K., Verheijen M. A. W., 2015, MNRAS, 448, 1715
Jaffé Y. L., et al., 2018, MNRAS, 476, 4753
Kenney J. D. P., Koopmann R. A., 1999, AJ, 117, 181
Kenney J. D. P., Geha M., Jáchym P., Crowl H. H., Dague W., Chung A., van Gorkom J., Vollmer B., 2014, ApJ, 780, 119
Kennicutt Robert C. J., 1998, ARA&A, 36, 189
Kozmanyan A., Bourdin H., Mazzotta P., Rasia E., Sereno M., 2019, A&A, 621, A34
Larson R. B., Tinsley B. M., Caldwell C. N., 1980, ApJ, 237, 692
Mahajan S., Mamon G. A., Raychaudhury S., 2011, MNRAS, 416, 2882
Mateus A., Sodré L., Cid Fernandes R., Stasińska G., Schoenell W., Gomes J. M., 2006, MNRAS, 370, 721
Moretti A., et al., 2018, MNRAS, 475, 4055
Moretti A., et al., 2020a, ApJ, 889, 9
Moretti A., et al., 2020b, ApJ, 897, L30
Müller A., et al., 2021, Nature Astronomy, 5, 159
O'Donnell J. E., 1994, ApJ, 422, 158
Poggianti B. M., et al., 2016a, in Napolitano N. R., Longo G., Marconi M., Paolillo M., Iodice E., eds, Vol. 42, The Universe of Digital Sky Surveys. p. 177, doi:10.1007/978-3-319-19330-4_28
Poggianti B. M., et al., 2016b, AJ, 151, 78
Poggianti B. M., et al., 2017, ApJ, 844, 48
Poggianti B. M., et al., 2019, MNRAS, 482, 4466
Ramatsoku M., et al., 2019, MNRAS, 487, 4580
Ramatsoku M., et al., 2020, A&A, 640, A22
Rhee J., Smith R., Choi H., Yi S. K., Jaffé Y., Candlish G., Sánchez-Jánssen R., 2017, ApJ, 843, 128
Roman-Oliveira F. V., Chies-Santos A. L., Rodríguez del Pino B., Aragón-Salamanca A., Gray M. E., Bamford S. P., 2019, MNRAS, 484, 892
Roman-Oliveira F., Chies-Santos A. L., Ferrari F., Lucatelli G., Rodríguez Del Pino B., 2021, MNRAS, 500, 40
Ruggiero R., Machado R. E. G., Roman-Oliveira F. V., Chies-Santos A. L., Lima Neto G. B., Doubrawa L., Rodríguez del Pino B., 2019, MNRAS, 484, 906
Schlegel D. J., Finkbeiner D. P., Davis M., 1998, ApJ, 500, 525
Sheen Y.-K., et al., 2017, ApJ, 840, L7
Strateva I., et al., 2001, AJ, 122, 1861
Vulcani B., et al., 2018, ApJ, 866, L25
Vulcani B., et al., 2020, ApJ, 899, 98
Wright E. L., 2006, PASP, 118, 1711
Yun K., et al., 2018, Monthly Notices of the Royal Astronomical Society, 483, 1042

APPENDIX A: MAPS OF ENTIRE SAMPLE

In this section we present maps of mean stellar ages and metallicities, both weighted by light, logarithm of H_α flux and star formation rate density, as done in Figure 1, for the other 18 galaxies in the sample.

This paper has been typeset from a TEX/LATEX file prepared by the author.

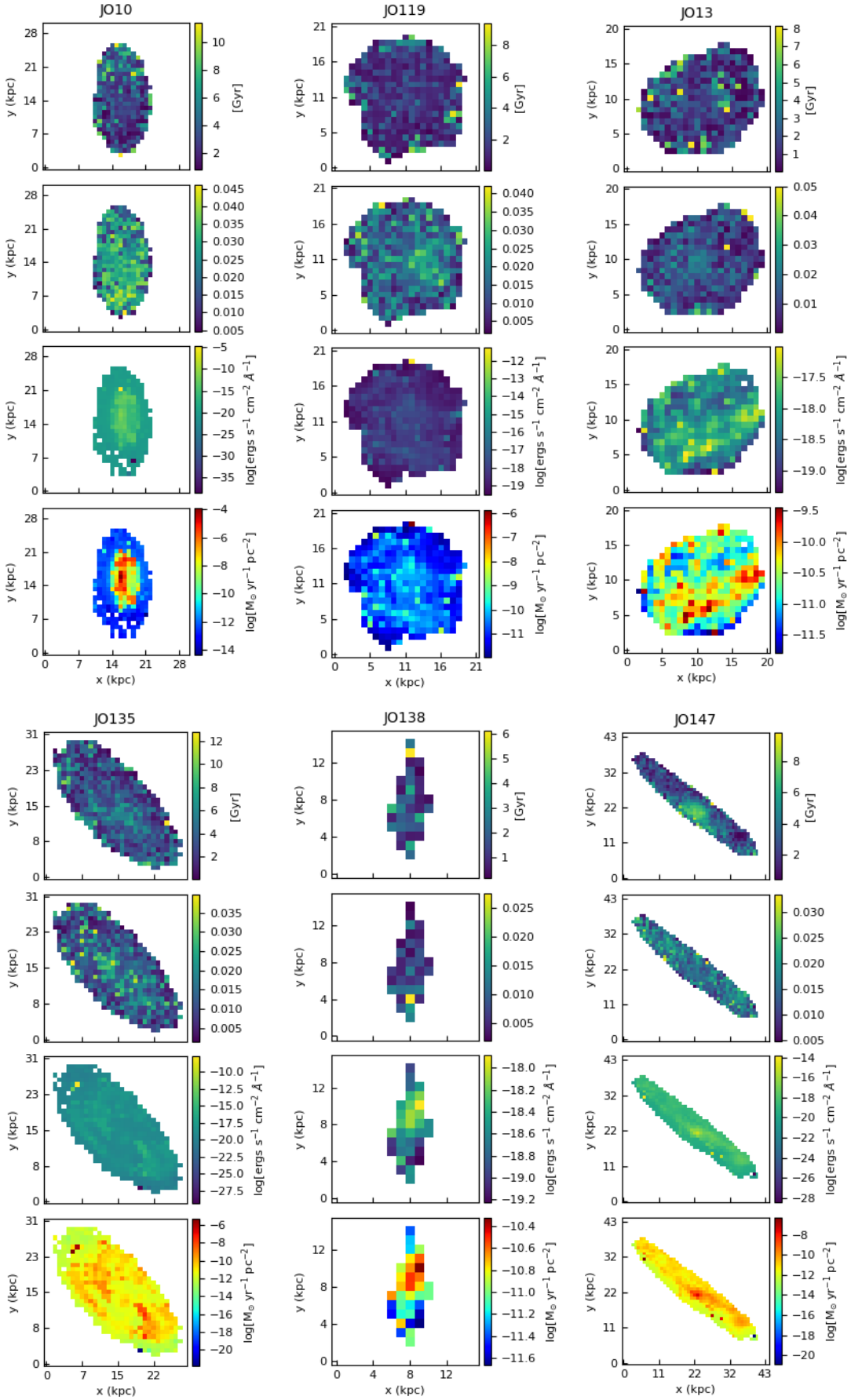
JO10
JO119
JO13
JO135
JO138
JO147
y (kpc)
x (kpc)
[Gyr]
log[ergs s^{-1} cm^{-2} Å^{-1}]
log[M$_\odot$ yr^{-1} pc^{-2}]

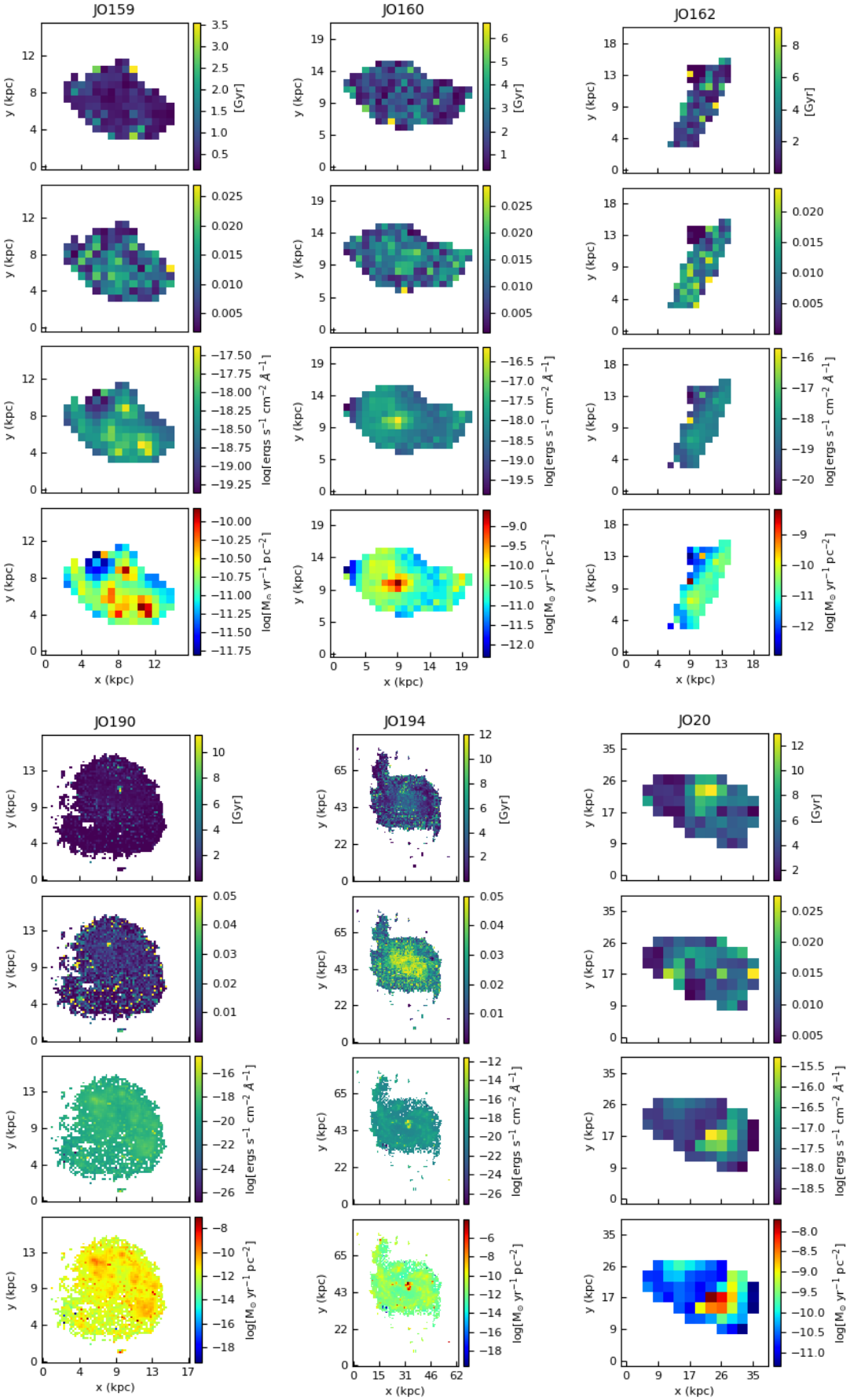
JO159
JO160
JO162
JO190
JO194
JO20
y (kpc)
x (kpc)
[Gyr]
log[ergs s^{-1} cm^{-2} Å^{-1}]
log[M$_\odot$ yr^{-1} pc^{-2}]

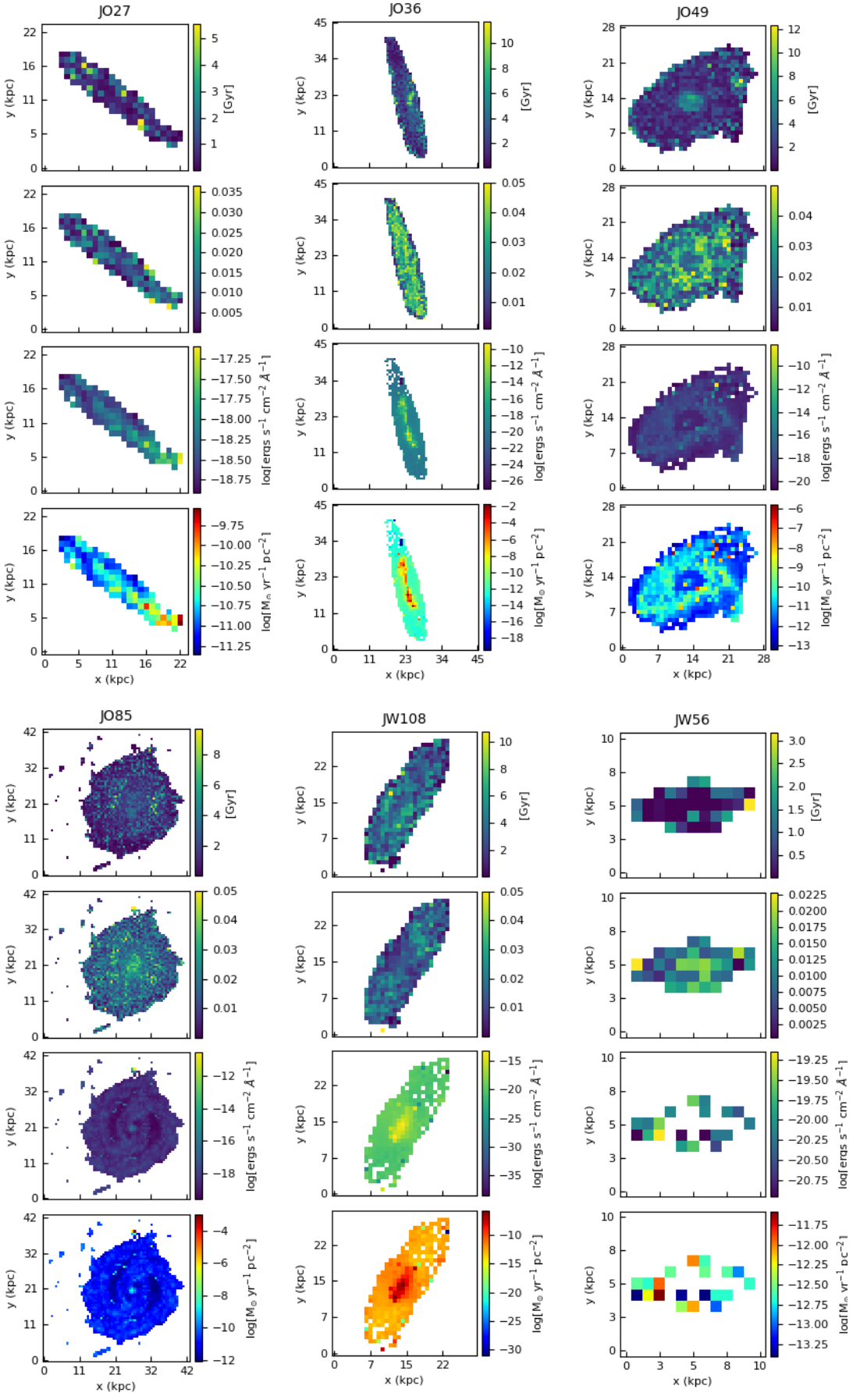
JO27
JO36
JO49
JO85
JW108
JW56
y (kpc)
x (kpc)
[Gyr]
log[ergs s^{-1} cm^{-2} Å^{-1}]
log[M$_\odot$ yr^{-1} pc^{-2}]

Chapter 4

Summary and concluding remarks

Our knowledge about extragalactic astrophysics has improved in giant steps along the past century, but still, many questions remain unsolved. In the last twenty years, it is noticeable a growing interest of astronomers in the problem of ram pressure stripping phenomenon and jellyfish galaxies. It was just in the past decade that large catalogs were made possible with observations of dozens of such objects.

However, there is no study of jellyfish galaxies using stellar population synthesis with self-consistency in nebular emission in the literature until now. Using the spectral population synthesis code FADO and high-resolution MUSE observations, we were able to implement spatially resolved stellar populations synthesis of 19 galaxies with the nebular emission additional constraint. Through those methods, we:

- created 2D morphology maps of mean stellar ages and metallicities, H_α emission, and "instantaneous" SFR surface densities;
- obtained SFHs of the galaxies and the sample as a whole, presented in the form of cumulative histograms and a table;
- confirmed through synthesis that there is recent star formation occurring in jellyfish galaxies;
- found an apparent anti-correlation between galaxies' mean ages and intensity of stripping;
- found that J5 and J4 galaxies are on average less metallic than the J3 ones (intermediary cases), while the J2 and J1 galaxies (weaker cases) have mean metallicities lower or similar to J3;

- found a pattern of the mean stellar ages based in the phase space, where jellyfish in the virialized region of the cluster have mean ages typically greater than those in the recent infall region ($t_{light} \gtrsim 2$ Gyr and $t_{mass} \gtrsim 3$ Gyr).

Unfortunately, our sample has been much reduced from the original 94 GASP galaxies due to their low continuum S/N in the tails, which is very disadvantageous to the reliability of synthesis. Future similar studies with larger samples would be more "ideal" to improve the accuracy of our statistical analysis. Also, a possible improvement to the work would be to consider the spatial correlation between neighbor spaxels and to smooth maps via Gaussian Markov random fields (González-Gaitán et al., 2019).

As shown in chapter 3 we aim to publish this work in a peer-reviewed journal of the area. The student will dedicate the initial phase of his Ph.D. to finish this research. Besides improving the discussion upon the already existing results, we are currently performing calculations of star formation rate along time and star formation acceleration (Martin et al., 2017), which is a measurement of the rapidity of SFR growth/decrease and is defined as $SFA \equiv d(NUV - i)_0/dt$, where NUV and i are magnitudes on GALEX near-ultraviolet filter and SDSS near-infrared filter, respectively. With such analysis, we hope to shed light on the understanding of bursting or quenching of jellyfish galaxies.

Also, there are three galaxies among our sample which have a post-stripping morphology, i.e., have an H_α disk smaller than the stellar one, and are believed to be in the final stages of RPS, since they quenched the star formation in the outskirts. We intend to separate the regions with and without H_α emission and compare their SFHs, on an attempt to understand better the timescales of the process.

References

[1] ALAVI, M., RAZMI, H. On the tidal evolution and tails formation of disc galaxies. , v. 360, p. 26, November 2015.

[2] BACON, R., ACCARDO, M., ADJALI, L., ANWAND, H., BAUER, S., BISWAS, I., BLAIZOT, J., BOUDON, D., BRAU-NOGUE, S., BRINCHMANN, J., CAILLIER, P., CAPOANI, L., CAROLLO, C. M., CONTINI, T., COUDERC, P., DAGUISÉ, E., DEIRIES, S., DELABRE, B., DREIZLER, S., DUBOIS, J., DUPIEUX, M., DUPUY, C., EMSELLEM, E., FECHNER, T., FLEISCHMANN, A., FRANÇOIS, M., GALLOU, G., GHARSA, T., GLINDEMANN, A., GOJAK, D., GUIDERDONI, B., HANSALI, G., HAHN, T., JARNO, A., KELZ, A., KOEHLER, C., KOSMALSKI, J., LAURENT, F., LE FLOCH, M., LILLY, S. J., LIZON, J. L., LOUPIAS, M., MANESCAU, A., MONSTEIN, C., NICKLAS, H., OLAYA, J. C., PARES, L., PASQUINI, L., PÉCONTAL-ROUSSET, A., PELLÓ, R., PETIT, C., POPOW, E., REISS, R., REMILLIEUX, A., RENAULT, E., ROTH, M., RUPPRECHT, G., SERRE, D., SCHAYE, J., SOUCAIL, G., STEINMETZ, M., STREICHER, O., STUIK, R., VALENTIN, H., VERNET, J., WEILBACHER, P., WISOTZKI, L., YERLE, N. The MUSE second-generation VLT instrument. In: GROUND-BASED AND AIRBORNE INSTRUMENTATION FOR ASTRONOMY III, McLean, Ian S., Ramsay, Suzanne K., Takami, Hideki, editores, v. 7735 of **Society of Photo-Optical Instrumentation Engineers (SPIE) Conference Series**, p. 773508, July 2010.

[3] BEKKI, KENJI. Unequal-Mass Galaxy Mergers and the Creation of Cluster S0 Galaxies. , v. 502, n. 2, p. L133–L137, August 1998.

[4] BELL, E. F., WOLF, C., MCINTOSH, D. H., COMBO-17 TEAM, , GEMS COLLABORATION, . Ten Billion Years of Early-Type Galaxy Evolution with COMBO-17 and GEMS. In: AMERICAN ASTRONOMICAL SOCI-

ETY MEETING ABSTRACTS, v. 203 of **American Astronomical Society Meeting Abstracts**, p. 131.05, December 2003.

[5] BELLHOUSE, C., JAFFÉ, Y. L., HAU, G. K. T., MCGEE, S. L., POGGIANTI, B. M., MORETTI, A., GULLIEUSZIK, M., BETTONI, D., FASANO, G., D'ONOFRIO, M. GASP. II. A MUSE View of Extreme Ram-Pressure Stripping along the Line of Sight: Kinematics of the Jellyfish Galaxy JO201. , v. 844, n. 1, p. 49, Jul 2017.

[6] BELLHOUSE, CALLUM, JAFFÉ, Y. L., MCGEE, S. L., POGGIANTI, B. M., SMITH, R., TONNESEN, S., FRITZ, J., HAU, G. K. T., GULLIEUSZIK, M., VULCANI, B. GASP. XV. A MUSE view of extreme ram-pressure stripping along the line of sight: physical properties of the jellyfish galaxy JO201. , v. 485, n. 1, p. 1157–1170, May 2019.

[7] BOSELLI, A., CUILLANDRE, J. C., FOSSATI, M., BOISSIER, S., BOMANS, D., CONSOLANDI, G., ANSELMI, G., CORTESE, L., CÔTÉ, P., DURRELL, P., FERRARESE, L., FUMAGALLI, M., GAVAZZI, G., GWYN, S., HENSLER, G., SUN, M., TOLOBA, E. Spectacular tails of ionized gas in the Virgo cluster galaxy NGC 4569. , v. 587, p. A68, March 2016.

[8] BOURNAUD, F., JOG, C. J., COMBES, F. Multiple minor mergers: formation of elliptical galaxies and constraints for the growth of spiral disks. , v. 476, n. 3, p. 1179–1190, December 2007.

[9] BRUZUAL, G., CHARLOT, S. Stellar population synthesis at the resolution of 2003. , v. 344, n. 4, p. 1000–1028, October 2003.

[10] CALVI, ROSA, POGGIANTI, BIANCA M., VULCANI, BENEDETTA. The Padova-Millennium Galaxy and Group Catalogue (PM2GC): the group-finding method and the PM2GC catalogues of group, binary and single field galaxies. , v. 416, n. 1, p. 727–738, Sep 2011.

[11] CALZETTI, DANIELA, ARMUS, LEE, BOHLIN, RALPH C., KINNEY, ANNE L., KOORNNEEF, JAN, STORCHI-BERGMANN, THAISA. The Dust Content and Opacity of Actively Star-forming Galaxies. , v. 533, n. 2, p. 682–695, April 2000.

[12] CAMPITIELLO, M. GIULIA, IGNESTI, ALESSANDRO, GITTI, MYRIAM, BRIGHENTI, FABRIZIO, RADOVICH, MARIO, WOLTER, ANNA,

TOMIČIĆ, NEVEN, BELLHOUSE, CALLUM, POGGIANTI, BIANCA M., MORETTI, ALESSIA, VULCANI, BENEDETTA, JAFFÉ, YARA L., PALADINO, ROSITA, MÜLLER, ANCLA, FRITZ, JACOPO, LOURENÇO, ANA C. C., GULLIEUSZIK, MARCO. GASP XXXIV: Unfolding the Thermal Side of Ram Pressure Stripping in the Jellyfish Galaxy JO201. , v. 911, n. 2, p. 144, April 2021.

[13] CARDELLI, JASON A., CLAYTON, GEOFFREY C., MATHIS, JOHN S. The Determination of Ultraviolet Extinction from the Optical and Near-Infrared. , v. 329, p. L33, June 1988.

[14] CARDOSO, LEANDRO S. M., GOMES, JEAN MICHEL, PAPADEROS, POLYCHRONIS. Self-consistent population spectral synthesis with FADO. I. The importance of nebular emission in modelling star-forming galaxies. , v. 622, p. A56, February 2019.

[15] CARROLL, BRADLEY W., OSTLIE, DALE A. **An Introduction to Modern Astrophysics**. 2nd.ed.: 2017.

[16] CHABRIER, GILLES. Galactic Stellar and Substellar Initial Mass Function. , v. 115, n. 809, p. 763–795, Jul 2003.

[17] DRESSLER, A. Galaxy morphology in rich clusters: implications for the formation and evolution of galaxies. , v. 236, p. 351–365, March 1980.

[18] DRESSLER, ALAN, OEMLER, JR., AUGUSTUS, COUCH, WARRICK J., SMAIL, IAN, ELLIS, RICHARD S., BARGER, AMY, BUTCHER, HARVEY, POGGIANTI, BIANCA M., SHARPLES, RAY M. Evolution since z = 0.5 of the Morphology-Density Relation for Clusters of Galaxies. , v. 490, n. 2, p. 577–591, December 1997.

[19] DRINKWATER, M. J., JONES, J. B., GREGG, M. D., PHILLIPPS, S. Compact Stellar Systems in the Fornax Cluster: Super-massive Star Clusters or Extremely Compact Dwarf Galaxies? , v. 17, n. 3, p. 227–233, December 2000.

[20] FASANO, GIOVANNI, POGGIANTI, BIANCA M., COUCH, WARRICK J., BETTONI, DANIELA, KJæRGAARD, PER, MOLES, MARIANO. The Evolution of the Galactic Morphological Types in Clusters. , v. 542, n. 2, p. 673–683, October 2000.

[21] FOSSATI, M., MENDEL, J. T., BOSELLI, A., CUILLAND RE, J. C., VOLLMER, B., BOISSIER, S., CONSOLANDI, G., FERRARESE, L., GWYN, S., AMRAM, P. A Virgo Environmental Survey Tracing Ionised Gas Emission (VESTIGE). II. Constraining the quenching time in the stripped galaxy NGC 4330. , v. 614, p. A57, Jun 2018.

[22] FRANCHETTO, ANDREA, VULCANI, BENEDETTA, POGGIANTI, BIANCA M., GULLIEUSZIK, MARCO, MINGOZZI, MATILDE, MORETTI, ALESSIA, TOMIČIĆ, NEVEN, FRITZ, JACOPO, BETTONI, DANIELA, JAFFÉ, YARA L. GASP XXVII: Gas-phase Metallicity Scaling Relations in Disk Galaxies with and without Ram Pressure Stripping. , v. 895, n. 2, p. 106, June 2020.

[23] FRITZ, JACOPO, MORETTI, ALESSIA, GULLIEUSZIK, MARCO, POGGIANTI, BIANCA, BRUZUAL, GUSTAVO, VULCANI, BENEDETTA, NICASTRO, FABRIZIO, JAFFÉ, YARA, CERVANTES SODI, BERNARDO, BETTONI, DANIELA. GASP. III. JO36: A Case of Multiple Environmental Effects at Play? , v. 848, n. 2, p. 132, Oct 2017.

[24] GAVAZZI, G., FUMAGALLI, M., CUCCIATI, O., BOSELLI, A. A snapshot on galaxy evolution occurring in the Great Wall: the role of Nurture at z = 0. , v. 517, p. A73, July 2010.

[25] GOMES, J. M., PAPADEROS, P. Fitting Analysis using Differential evolution Optimization (FADO):. Spectral population synthesis through genetic optimization under self-consistency boundary conditions. , v. 603, p. A63, July 2017.

[26] GONZÁLEZ-GAITÁN, S., DE SOUZA, R. S., KRONE-MARTINS, A., CAMERON, E., COELHO, P., GALBANY, L., ISHIDA, E. E. O., COIN COLLABORATION, . Spatial field reconstruction with INLA: application to IFU galaxy data. , v. 482, n. 3, p. 3880–3891, January 2019.

[27] GULLIEUSZIK, MARCO, POGGIANTI, BIANCA M., MCGEE, SEAN L., MORETTI, ALESSIA, VULCANI, BENEDETTA, TONNESEN, STEPHANIE, ROEDIGER, ELKE, JAFFÉ, YARA L., FRITZ, JACOPO, FRANCHETTO, ANDREA, OMIZZOLO, ALESSANDRO, BETTONI, DANIELA, RADOVICH, MARIO, WOLTER, ANNA. GASP. XXI. Star Formation Rates in the Tails of Galaxies Undergoing Ram Pressure Stripping. , v. 899, n. 1, p. 13, August 2020.

[28] GULLIEUSZIK, MARCO, POGGIANTI, BIANCA M., MORETTI, ALESSIA, FRITZ, JACOPO, JAFFÉ, YARA L., HAU, GEORGE, BISCHKO, JAN C., BELLHOUSE, CALLUM, BETTONI, DANIELA, FASANO, GIOVANNI. Erratum: "GASP .IV. A Muse View of Extreme Ram-pressure Stripping in the Plane of the Sky: The Case of Jellyfish Galaxy JO204" (¡A href="http://doi.org/10.3847/1538-4357/aa8322"¿2017, ApJ, 846, 27¡/A¿). , v. 853, n. 2, p. 199, Feb 2018.

[29] GUNN, JAMES E., GOTT, III, J. RICHARD. On the Infall of Matter Into Clusters of Galaxies and Some Effects on Their Evolution. , v. 176, p. 1, August 1972.

[30] HAYNES, MARTHA P., GIOVANELLI, RICARDO, CHINCARINI, GUIDO L. The Influence of Envirionment on the H I Content of Galaxies. , v. 22, p. 445–470, Jan 1984.

[31] HEWLETT, TIMOTHY, VILLFORTH, CAROLIN, WILD, VIVIENNE, MENDEZ-ABREU, JAIRO, PAWLIK, MILENA, ROWLANDS, KATE. The redshift evolution of major merger triggering of luminous AGNs: a slight enhancement at z $\sim$ 2. , v. 470, n. 1, p. 755–770, September 2017.

[32] HILKER, M., INFANTE, L., RICHTLER, T. The central region of the Fornax cluster. III. Dwarf galaxies, globular clusters, and cD halo - are there interrelations? , v. 138, p. 55–70, July 1999.

[33] HUBBLE, EDWIN. No. 324. Extra-galactic nebulae. **Contributions from the Mount Wilson Observatory / Carnegie Institution of Washington**, v. 324, p. 1–49, January 1926.

[34] HUBBLE, EDWIN P. Ngc 6822, a remote stellar system. **The Astrophysical Journal**, v. 62, 1925.

[35] JAFFÉ, YARA L., POGGIANTI, BIANCA M., MORETTI, ALESSIA, GULLIEUSZIK, MARCO, SMITH, RORY, VULCANI, BENEDETTA, FASANO, GIOVANNI, FRITZ, JACOPO, TONNESEN, STEPHANIE, BETTONI, DANIELA, HAU, GEORGE, BIVIANO, ANDREA, BELLHOUSE, CALLUM, MCGEE, SEAN. GASP. IX. Jellyfish galaxies in phase-space: an orbital study of intense ram-pressure stripping in clusters. , v. 476, n. 4, p. 4753–4764, Jun 2018.

[36] JAFFÉ, YARA L., SMITH, RORY, CANDLISH, GRAEME N., POGGIANTI, BIANCA M., SHEEN, YUN-KYEONG, VERHEIJEN, MARC A. W. BUDHIES II: a phase-space view of H I gas stripping and star formation quenching in cluster galaxies. , v. 448, n. 2, p. 1715–1728, Apr 2015.

[37] KAVIRAJ, S., KHOCHFAR, S., SCHAWINSKI, K., YI, S. K., GAWISER, E., SILK, J., VIRANI, S. N., CARDAMONE, C. N., VAN DOKKUM, P. G., URRY, C. M. The UV colours of high-redshift early-type galaxies: evidence for recent star formation and stellar mass assembly over the last 8 billion years. , v. 388, n. 1, p. 67–79, July 2008.

[38] KENNEY, J., KOOPMANN, R. Ongoing Gas Stripping in the Virgo Cluster Spiral NGC 4522. In: AMERICAN ASTRONOMICAL SOCIETY MEETING ABSTRACTS, v. 191, p. 116.03, Dec 1997.

[39] KENNEY, JEFFREY D. P., GEHA, MARLA, JÁCHYM, PAVEL, CROWL, HUGH H., DAGUE, WILLIAM, CHUNG, AEREE, VAN GORKOM, JACQUELINE, VOLLMER, BERND. Transformation of a Virgo Cluster Dwarf Irregular Galaxy by Ram Pressure Stripping: IC3418 and Its Fireballs. , v. 780, n. 2, p. 119, Jan 2014.

[40] KENNEY, JEFFREY D. P., KOOPMANN, REBECCA A. Ongoing Gas Stripping in the Virgo Cluster Spiral Galaxy NGC 4522. , v. 117, n. 1, p. 181–189, Jan 1999.

[41] KENNICUTT, JR., ROBERT C. Star Formation in Galaxies Along the Hubble Sequence. , v. 36, p. 189–232, January 1998.

[42] KOZMANYAN, ARPINE, BOURDIN, HERVÉ, MAZZOTTA, PASQUALE, RASIA, ELENA, SERENO, MAURO. Deriving the Hubble constant using Planck and XMM-Newton observations of galaxy clusters. , v. 621, p. A34, January 2019.

[43] LAMBAS, D. G., ALONSO, S., MESA, V., O'MILL, A. L. Galaxy interactions. I. Major and minor mergers. , v. 539, p. A45, March 2012.

[44] LARSON, R. B., TINSLEY, B. M., CALDWELL, C. N. The evolution of disk galaxies and the origin of S0 galaxies. , v. 237, p. 692–707, May 1980.

[45] LIN, LIHWAI, COOPER, MICHAEL C., JIAN, HUNG-YU, KOO, DAVID C., PATTON, DAVID R., YAN, RENBIN, WILLMER, CHRISTOPHER N. A.,

COIL, ALISON L., CHIUEH, TZIHONG, CROTON, DARREN J., GERKE, BRIAN F., LOTZ, JENNIFER, GUHATHAKURTA, PURAGRA, NEWMAN, JEFFREY A. Where do Wet, Dry, and Mixed Galaxy Mergers Occur? A Study of the Environments of Close Galaxy Pairs in the DEEP2 Galaxy Redshift Survey. , v. 718, n. 2, p. 1158–1170, August 2010.

[46] MAHAJAN, SMRITI, MAMON, GARY A., RAYCHAUDHURY, SOMAK. The velocity modulation of galaxy properties in and near clusters: quantifying the decrease in star formation in backsplash galaxies. , v. 416, n. 4, p. 2882–2902, October 2011.

[47] MARTIN, D. CHRISTOPHER, GONÇALVES, THIAGO S., DARVISH, BEHNAM, SEIBERT, MARK, SCHIMINOVICH, DAVID. Quenching or Bursting: Star Formation Acceleration—A New Methodology for Tracing Galaxy Evolution. , v. 842, n. 1, p. 20, June 2017.

[48] MO, HOUJUN, BOSCH, FRANK VAN DEN, WHITE, SIMON. **Galaxy Formation and Evolution**. Illustrated edition.ed.: 2010.

[49] MOORE, BEN, KATZ, NEAL, LAKE, GEORGE, DRESSLER, ALAN, OEMLER, AUGUSTUS. Galaxy harassment and the evolution of clusters of galaxies. , v. 379, n. 6566, p. 613–616, February 1996.

[50] MORETTI, A., POGGIANTI, B. M., GULLIEUSZIK, M., MAPELLI, M., JAFFÉ, Y. L., FRITZ, J., BIVIANO, A., FASANO, G., BETTONI, D., VULCANI, B. GASP. V. Ram-pressure stripping of a ring Hoag's-like galaxy in a massive cluster. , v. 475, n. 3, p. 4055–4065, Apr 2018.

[51] MORETTI, ALESSIA, PALADINO, ROSITA, POGGIANTI, BIANCA M., SERRA, PAOLO, RAMATSOKU, MPATI, FRANCHETTO, ANDREA, DEB, TIRNA, GULLIEUSZIK, MARCO, TOMIČIĆ, NEVEN, MINGOZZI, MATILDE, VULCANI, BENEDETTA, RADOVICH, MARIO, BETTONI, DANIELA, FRITZ, JACOPO. The High Molecular Gas Content, and the Efficient Conversion of Neutral into Molecular Gas, in Jellyfish Galaxies. , v. 897, n. 2, p. L30, July 2020a.

[52] MORETTI, ALESSIA, PALADINO, ROSITA, POGGIANTI, BIANCA M., SERRA, PAOLO, ROEDIGER, ELKE, GULLIEUSZIK, MARCO, TOMIČIĆ, NEVEN, RADOVICH, MARIO, VULCANI, BENEDETTA, JAFFÉ, YARA L., FRITZ, JACOPO, BETTONI, DANIELA, RAMATSOKU,

MPATI, WOLTER, ANNA. GASP. XXII. The Molecular Gas Content of the JW100 Jellyfish Galaxy at z $\sim$ 0.05: Does Ram Pressure Promote Molecular Gas Formation? , v. 889, n. 1, p. 9, January 2020b.

[53] MULLAN, B., CHARLTON, J. C., KONSTANTOPOULOS, I. S., BASTIAN, N., CHANDAR, R., DURRELL, P. R., ELMEGREEN, D., ENGLISH, J., GALLAGHER, S. C., GRONWALL, C., HIBBARD, J. E., HUNSBERGER, S., JOHNSON, K. E., KEPLEY, A., KNIERMAN, K., KORIBALSKI, B., LEE, K. H., MAYBHATE, A., PALMA, C., VACCA, W. D. Tidal Tails in Interacting Galaxies: Formation of Compact Stellar Structures. In: GALAXY WARS: STELLAR POPULATIONS AND STAR FORMATION IN INTERACTING GALAXIES, Smith, B., Higdon, J., Higdon, S., Bastian, N., editores, v. 423 of **Astronomical Society of the Pacific Conference Series**, p. 129, June 2010.

[54] MÜLLER, ANCLA, POGGIANTI, BIANCA MARIA, PFROMMER, CHRISTOPH, ADEBAHR, BJÖRN, SERRA, PAOLO, IGNESTI, ALESSANDRO, SPARRE, MARTIN, GITTI, MYRIAM, DETTMAR, RALF-JÜRGEN, VULCANI, BENEDETTA, MORETTI, ALESSIA. Highly ordered magnetic fields in the tail of the jellyfish galaxy JO206. **Nature Astronomy**, v. 5, p. 159–168, January 2021.

[55] OSTERBROCK, DONALD, FERLAND, GARY. **Astrophysics of Gaseous Nebulae and Active Galactic Nuclei**. 1st edition.ed.: 2006.

[56] PERLMUTTER, S., ALDERING, G., GOLDHABER, G., KNOP, R. A., NUGENT, P., CASTRO, P. G., DEUSTUA, S., FABBRO, S., GOOBAR, A., GROOM, D. E., HOOK, I. M., KIM, A. G., KIM, M. Y., LEE, J. C., NUNES, N. J., PAIN, R., PENNYPACKER, C. R., QUIMBY, R., LIDMAN, C., ELLIS, R. S., IRWIN, M., MCMAHON, R. G., RUIZ-LAPUENTE, P., WALTON, N., SCHAEFER, B., BOYLE, B. J., FILIPPENKO, A. V., MATHESON, T., FRUCHTER, A. S., PANAGIA, N., NEWBERG, H. J. M., COUCH, W. J., PROJECT, THE SUPERNOVA COSMOLOGY. Measurements of Ω and Λ from 42 High-Redshift Supernovae. , v. 517, n. 2, p. 565–586, June 1999.

[57] POGGIANTI, B. M., FASANO, G., BETTONI, D., CAVA, A., COUCH, W., D'ONOFRIO, M., DRESSLER, A., FRITZ, J., KJAERGAARD, P., GULLIEUSZIK, M. The Wide-Field Nearby Galaxy-Cluster Survey (WINGS) and Its Extension OMEGAWINGS. In: THE UNIVERSE OF DIGITAL SKY

SURVEYS, Napolitano, Nicola R., Longo, Giuseppe, Marconi, Marcella, Paolillo, Maurizio, Iodice, Enrichetta, editores, v. 42, p. 177, Jan 2016a.

[58] POGGIANTI, B. M., FASANO, G., OMIZZOLO, A., GULLIEUSZIK, M., BETTONI, D., MORETTI, A., PACCAGNELLA, A., JAFFÉ, Y. L., VULCANI, B., FRITZ, J., COUCH, W., D'ONOFRIO, M. Jellyfish Galaxy Candidates at Low Redshift. , v. 151, n. 3, p. 78, March 2016b.

[59] POGGIANTI, BIANCA M., GULLIEUSZIK, MARCO, TONNESEN, STEPHANIE, MORETTI, ALESSIA, VULCANI, BENEDETTA, RADOVICH, MARIO, JAFFÉ, YARA, FRITZ, JACOPO, BETTONI, DANIELA, FRANCHETTO, ANDREA. GASP XIII. Star formation in gas outside galaxies. , v. 482, n. 4, p. 4466–4502, Feb 2019.

[60] POGGIANTI, BIANCA M., JAFFÉ, YARA L., MORETTI, ALESSIA, GULLIEUSZIK, MARCO, RADOVICH, MARIO, TONNESEN, STEPHANIE, FRITZ, JACOPO, BETTONI, DANIELA, VULCANI, BENEDETTA, FASANO, GIOVANNI, BELLHOUSE, CALLUM, HAU, GEORGE, OMIZZOLO, ALESSANDRO. Ram-pressure feeding of supermassive black holes. , v. 548, n. 7667, p. 304–309, August 2017a.

[61] POGGIANTI, BIANCA M., MORETTI, ALESSIA, GULLIEUSZIK, MARCO, FRITZ, JACOPO, JAFFÉ, YARA, BETTONI, DANIELA, FASANO, GIOVANNI, BELLHOUSE, CALLUM, HAU, GEORGE, VULCANI, BENEDETTA. GASP. I. Gas Stripping Phenomena in Galaxies with MUSE. , v. 844, n. 1, p. 48, Jul 2017b.

[62] RADOVICH, MARIO, POGGIANTI, BIANCA, JAFFÉ, YARA L., MORETTI, ALESSIA, BETTONI, DANIELA, GULLIEUSZIK, MARCO, VULCANI, BENEDETTA, FRITZ, JACOPO. GASP - XIX. AGN and their outflows at the centre of jellyfish galaxies. , v. 486, n. 1, p. 486–503, June 2019.

[63] RHEE, JINSU, SMITH, RORY, CHOI, HOSEUNG, YI, SUKYOUNG K., JAFFÉ, YARA, CANDLISH, GRAEME, SÁNCHEZ-JÁNSSEN, RUBEN. Phase-space Analysis in the Group and Cluster Environment: Time Since Infall and Tidal Mass Loss. , v. 843, n. 2, p. 128, July 2017.

[64] RIESS, ADAM G., FILIPPENKO, ALEXEI V., CHALLIS, PETER, CLOCCHIATTI, ALEJANDRO, DIERCKS, ALAN, GARNAVICH, PETER M.,

GILLILAND, RON L., HOGAN, CRAIG J., JHA, SAURABH, KIRSHNER, ROBERT P., LEIBUNDGUT, B., PHILLIPS, M. M., REISS, DAVID, SCHMIDT, BRIAN P., SCHOMMER, ROBERT A., SMITH, R. CHRIS, SPYROMILIO, J., STUBBS, CHRISTOPHER, SUNTZEFF, NICHOLAS B., TONRY, JOHN. Observational Evidence from Supernovae for an Accelerating Universe and a Cosmological Constant. , v. 116, n. 3, p. 1009–1038, September 1998.

[65] ROMAN-OLIVEIRA, FERNANDA, CHIES-SANTOS, ANA L., FERRARI, FABRICIO, LUCATELLI, GEFERSON, RODRíGUEZ DEL PINO, BRUNO. Morphometry as a probe of the evolution of jellyfish galaxies: evidence of broadening in the surface brightness profiles of ram-pressure stripping candidates in the multicluster system A901/A902. , v. 500, n. 1, p. 40–53, January 2021.

[66] ROMAN-OLIVEIRA, FERNANDA V., CHIES-SANTOS, ANA L., RODRíGUEZ DEL PINO, BRUNO, ARAGÓN-SALAMANCA, A., GRAY, MEGHAN E., BAMFORD, STEVEN P. OMEGA-OSIRIS mapping of emission-line galaxies in A901/2-V. The rich population of jellyfish galaxies in the multicluster system Abell 901/2. , v. 484, n. 1, p. 892–905, Mar 2019.

[67] RUGGIERO, RAFAEL, MACHADO, RUBENS E. G., ROMAN-OLIVEIRA, FERNANDA V., CHIES-SANTOS, ANA L., LIMA NETO, GASTÃO B., DOUBRAWA, LIA, RODRíGUEZ DEL PINO, BRUNO. Galaxy cluster mergers as triggers for the formation of jellyfish galaxies: case study of the A901/2 system. , v. 484, n. 1, p. 906–914, March 2019.

[68] SCHOMBERT, JAMES M. The Structure of Brightest Cluster Members. II. Mergers. , v. 64, p. 643, August 1987.

[69] SHEEN, YUN-KYEONG, SMITH, RORY, JAFFÉ, YARA, KIM, MINJIN, YI, SUKYOUNG K., DUC, PIERRE-ALAIN, NANTAIS, JULIE, CANDLISH, GRAEME, DEMARCO, RICARDO, TREISTER, EZEQUIEL. Discovery of Ram-pressure Stripped Gas around an Elliptical Galaxy in Abell 2670. , v. 840, n. 1, p. L7, May 2017.

[70] SPRINGEL, VOLKER, WHITE, SIMON D. M., JENKINS, ADRIAN, FRENK, CARLOS S., YOSHIDA, NAOKI, GAO, LIANG, NAVARRO, JULIO, THACKER, ROBERT, CROTON, DARREN, HELLY, JOHN, PEACOCK,

JOHN A., COLE, SHAUN, THOMAS, PETER, COUCHMAN, HUGH, EVRARD, AUGUST, COLBERG, JÖRG, PEARCE, FRAZER. Simulations of the formation, evolution and clustering of galaxies and quasars. , v. 435, n. 7042, p. 629–636, June 2005.

[71] THOMAS, DANIEL, MARASTON, CLAUDIA, BENDER, RALF, MENDES DE OLIVEIRA, CLAUDIA. The Epochs of Early-Type Galaxy Formation as a Function of Environment. , v. 621, n. 2, p. 673–694, March 2005.

[72] TOOMRE, ALAR. Mergers and Some Consequences. In: EVOLUTION OF GALAXIES AND STELLAR POPULATIONS, Tinsley, Beatrice M., Larson, D. Campbell, Richard B. Gehret, editores, p. 401, January 1977.

[73] VULCANI, BENEDETTA, MORETTI, ALESSIA, POGGIANTI, BIANCA M., FASANO, GIOVANNI, FRITZ, JACOPO, GULLIEUSZIK, MARCO, DUC, PIERRE-ALAIN, JAFFÉ, YARA, BETTONI, DANIELA. GASP. VIII. Capturing the Birth of a Tidal Dwarf Galaxy in a Merging System at z 0.05. , v. 850, n. 2, p. 163, Dec 2017.

[74] VULCANI, BENEDETTA, POGGIANTI, BIANCA M., GULLIEUSZIK, MARCO, MORETTI, ALESSIA, TONNESEN, STEPHANIE, JAFFÉ, YARA L., FRITZ, JACOPO, FASANO, GIOVANNI, BETTONI, DANIELA. Enhanced Star Formation in Both Disks and Ram-pressure-stripped Tails of GASP Jellyfish Galaxies. , v. 866, n. 2, p. L25, Oct 2018.

[75] VULCANI, BENEDETTA, POGGIANTI, BIANCA M., TONNESEN, STEPHANIE, MCGEE, SEAN L., MORETTI, ALESSIA, FRITZ, JACOPO, GULLIEUSZIK, MARCO, JAFFÉ, YARA L., FRANCHETTO, ANDREA, TOMIČIĆ, NEVEN, MINGOZZI, MATILDE, BETTONI, DANIELA, WOLTER, ANNA. GASP XXX. The Spatially Resolved SFR-Mass Relation in Stripping Galaxies in the Local Universe. , v. 899, n. 2, p. 98, August 2020.

[76] WALCHER, JAKOB, GROVES, BRENT, BUDAVÁRI, TAMÁS, DALE, DANIEL. Fitting the integrated spectral energy distributions of galaxies. , v. 331, p. 1–52, January 2011.

[77] WITTMANN, CAROLIN, LISKER, THORSTEN, PASQUALI, ANNA, HILKER, MICHAEL, GREBEL, EVA K. Peculiar compact stellar systems in the Fornax cluster. , v. 459, n. 4, p. 4450–4466, July 2016.

[78] YUN, KIYUN, PILLEPICH, ANNALISA, ZINGER, ELAD, NELSON, DYLAN, DONNARI, MARTINA, JOSHI, GANDHALI, RODRIGUEZ-GOMEZ, VICENTE, GENEL, SHY, WEINBERGER, RAINER, VOGELSBERGER, MARK, HERNQUIST, LARS. Jellyfish galaxies with the IllustrisTNG simulations – I. Gas-stripping phenomena in the full cosmological context. **Monthly Notices of the Royal Astronomical Society**, v. 483, n. 1, p. 1042–1066, 11 2018.